Mineralia Slovaca, Web ISSN 1338-3523, ISSN 0369-2086
51 (2019), 1 – 30, © Authors 2019. CC BY 4.0

Postglacial deformation history of sackungen on the southern slope of Mount Chabenec, Nízke Tatry Mts., Slovakia

JAMES P. McCALPIN[1], PAVEL LIŠČÁK[2*], ROBERT JELÍNEK[3], MOLLY O. ZORBA[4] and NURIA SANTACANA[5]

[1] GEO-HAZ Consulting, Crestone, Colorado, USA
[2] State Geological Institute of Dionýz Štúr, Bratislava, Slovak Republic: pavel.liscak@geology.sk,
* *Corresponding author*
[3] State Geological Institute of Dionýz Štúr, Banská Bystrica, Slovak Republic
[4] Apex Companies LLC, Thousand Oaks, California, USA
[5] Universitat Politècnica de Catalunya, Barcelona, Spain

Abstract: A series of distinct antislope scarps crosses the southern slope of the Mt. Chabenec in the Nízke Tatry Mountain range. Previous studies assumed that the deep-seated deformation with features of creep movement developed slowly towards the Lomnistá dolina Valley in the south-east direction. The field exploration comprised four exploration trenches across the antislope scarps, which have revealed conspicuous mylonite zones dipping at 50° towards the North. Trenches across the troughs adjacent to the antislope scarps all contained colluvial wedges, fissure fills, fault truncations, and angular unconformities. These structures and 20 ^{14}C-ages on trough sediments and buried soils indicate the scarps were formed by episodic displacements over the past 9.6 ka. The most recent displacement event (MRE) on all three scarps overlaps in age between 1,410 to 1,860 cal years BP (2-sigma range). The Nízke Tatry Mountains do have a historic record of earthquake shaking, so the MRE at Mount Chabenec could have been triggered by similar ground motions.

Key words: sackungen, slope stability, gravitational spreading, seismicity, Nízke Tatry Mts.,

Graphical abstract

Highlights

- Paleoseizmic trenching techniques were applied in four trenches dug in 1997 across three antislope scarps of deep seated slope deformation on the south ridge of Mount Chabenec, Nízke Tatry Mts.
- Structure and stratigraphy exposed in the trenches are consistent with episodic slip on the sackungen faults coupled with episodic deposition and soil formation in the adjacent troughs.
- Radiocarbon ages indicate that in all four trenches, there was a displacement event in the late Holocene (shortly after 1,410 to 1,860 cal yrs BP).

Introduction

Mt. Chabenec (48.94°N, 19.49°E; elevation 1,959 m) is situated in the Low Tatras (Nízke Tatry) Mountains, Central Slovakia (Fig. 1), in Nízke Tatry National Park. The marked feature of Mt. Chabenec is a series of parallel antislope scarps on its southern slope, which descends to the Lomnistá Valley floor (1,300 m elevation). These antislope scarps were described decades ago by Jahn (1964), Nemčok (1972), and Mahr and Nemčok (1977). The Chabenec deformation is part of a longer belt of similar deformations developed between Chopok and Prašivá Hills (a distance of 25 km) within the granitoid massifs forming the main ridge of the Low Tatras Mountains (Nemčok, 1982). Approximately 38 % of the mountain ridge is affected by such deformation. The scarps are easy to see because most of the ridge lies above the tree line at ~1,400 m.

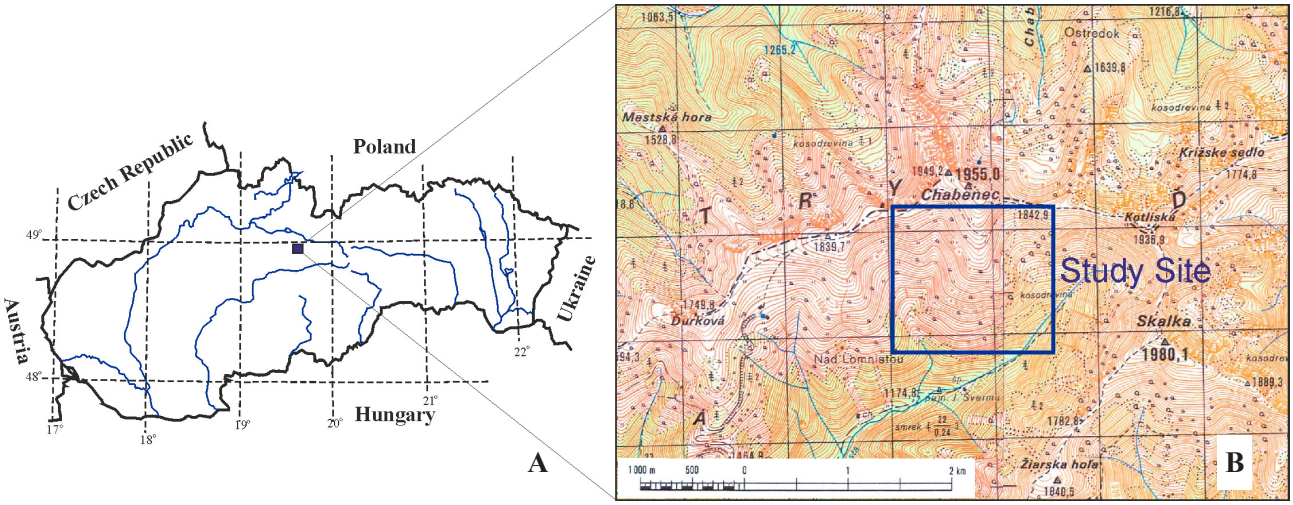

Fig. 1. Location map of the study site. A – shaded relief map of Slovak Republic and adjacent areas, dominated by the Carpathian Mountains. B – topographic map of the western part of the Nízke Tatry Mountains centered on Mt. Chabenec; thick contour interval is 50 m. Study site (box) occupies the southern slope of Mt. Chabenec.

This paper describes the results of a trenching study performed by the State Geological Institute of Dionýz Štúr (SGIDŠ) (formerly Geological Survey of the Slovak Republic), and the University of Colorado, USA. The study goal was to determine if paleoseismic trenching techniques could reconstruct the timing and rates of movements on these classic sackungen scarps. Prior to our 1997 field work few sackungen scarps had been trenched (e.g., Beget, 1985; McCalpin and Irvine, 1995; Thompson et al., 1997). However, in the past 20 years a steadily-increasing number of trenching investigations have been performed on sackungen (e.g., McCalpin and Hart, 2003; Tibaldi et al., 2004; Gutierrez et al., 2005, 2008; Agliardi et al., 2009; McCalpin et al., 2011; Pánek et al., 2011; Moro et al., 2012; Carbonel et al., 2013; Gori et al., 2014; Onida et al., 2016; Mariotto and Tibaldi, 2016) including in the Czech and Slovak Republics (Pánek et al., 2017).

Geological Setting

According to the geologic-geomorphologic division of Western Carpathians (Mazúr and Lukniš, 1980), Mt. Chabenec belongs to the Ďumbier part of the Low Tatras. This mountain range represents a core mountain and is a part of the Tatricum Unit. This unit is built of crystalline basement rocks and Late Palaeozoic and Mesozoic cover sedimentary rocks.The Mt. Chabenec site is underlain by crystalline rocks. It consists of two parts (Fig. 2):

The northern part of the slope up to the peak is composed of medium-grained biotitic granodiorites to tonalites of the Ďumbier type. On the southern rim of this part a narrow contact zone is developed, in which hybrid granitoids, as well as remains of the mantle (the biotitic gneisses, mainly) can be observed. In the NE part of this zone relatively thin bodies of leucocratic granitoids crop out. According to the latest radiometric dating the intrusive activity took place at about the Devonian-Carboniferous boundary.

The southern part of the slope (the head of the Lomnistá Valley) is built of banded augengneisses with porphyroblasts of K-feldspars several cm in diameter. The orthogneiss with layers of paragneiss and amphibolites prevails. A re-markable feature of these rocks are ductile deformation structures (foliation, folds).

The contact of the gneiss complex and granitoids follows the direction of the main ridge. Its cropping out in the field is due to relatively extensive Quaternary cover rather indiscernible. We suppose that this is a tectonic contact, with the general strike E-W. The tectonic juxtaposition of both complexes likely took place in the Hercynian orogeny, but the important tectonic failures of the crystalline developed during the Alpine tectogenesis stage, mainly. In this stage mylonite zones originated, following older structures or new fault structures. They are mostly of the NE-SW direction with a medium to steep strike towards SE. In most cases they are overthrusts and strike-slip faults. The transversal brittle NW-SE and N-W faults, normal faults mostly, do not show large displacement amplitude.

Methods

Trenching: We excavated four trenches with picks and shovels across sackungen troughs in the central part of the southern slope, between 1,625 and 1,750 m elevation (Fig. 3). Trenches were roughly 60 cm wide, 4.5 to 7.3 m long, and 2.0 to 2.7 m deep. The eastern wall of each trench was cleaned and gridded with string, after which we drew a subjective field trench log on graph paper at a scale of 1:15 using the manual method (McCalpin, 2013). Those

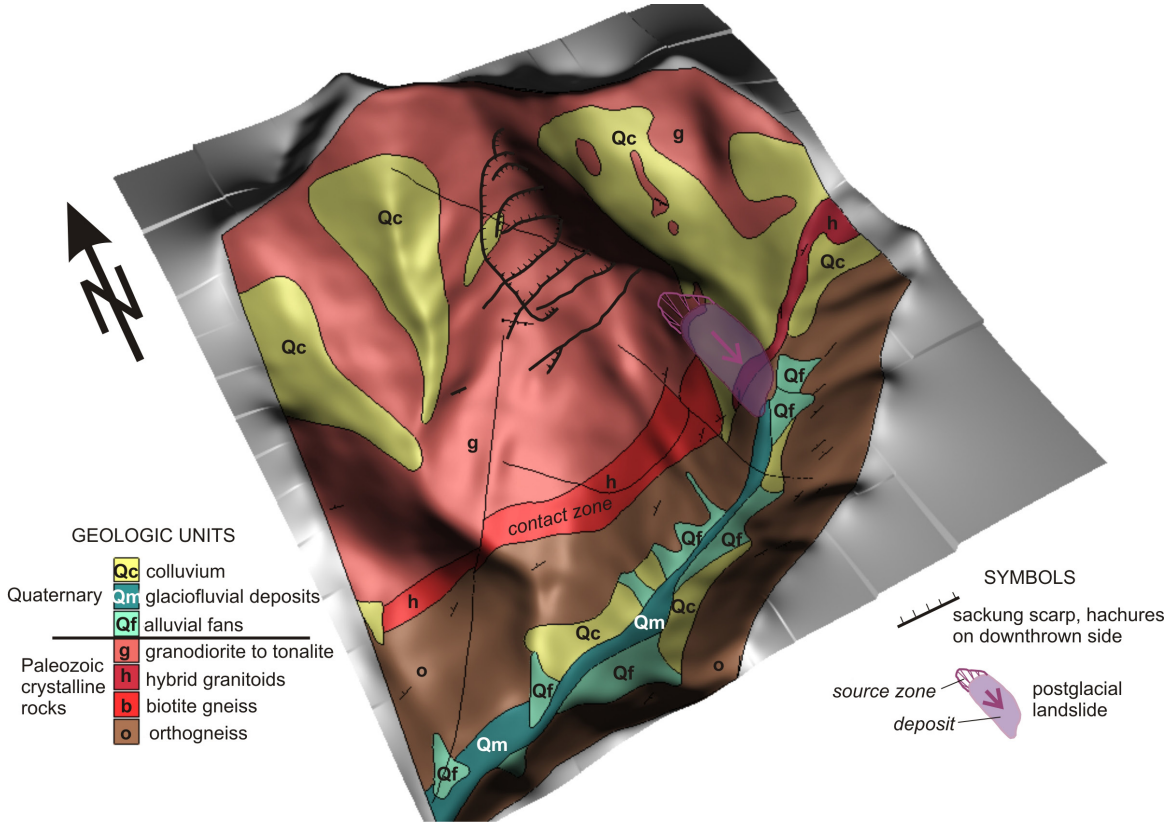

Fig. 2. Geologic map of the southeastern slope of Mt. Chabenec (Biely et al., 1992, modified, on DMR compiled by P. Pauditš). The antislope scarps are located relatively high on the southern slope of the mountain, on a subsidiary ridge flanked by two colluvium-filled valleys. Vertical relief between Mt. Chabenec and the Lomnistá Valley is 660 m.

logs were then digitized for this paper. Unconsolidated stratigraphic units were defined based on color, texture, and sedimentary structures. Soil horizons developed on deposits (parent materials) were also identified and labeled according to the A/B/C horizon terminology used in the USA (e.g., Soil Survey Staff, 2014).

Geochronology: The three trenches were located in parts of sackungen troughs that were closed (or nearly closed) topographic depressions, in hopes that fine-grained trough sediments would contain organics amenable to radiocarbon dating. Each trench did contain both datable organics, and carbon from the finer-grained deposits (e.g., sag-pond silts and clays) yielded age sequences in correct stratigraphic order. However, carbon found in coarser-grained deposits, in scarp-derived colluvium, and in shear zones often yielded ages out of stratigraphic order, as described under Trenches 2, 3, and 4. All samples were dated by accelerator mass spectrometry (AMS) at the National Science Foundation Accelerator Dating Facility at the University of Arizona. The calibration curve of Reimer et al. (2013) was used to convert radiocarbon years to calendar years.

Results

Geomorphology of Slope Deformation

The antislope scarps on the upper southern slope of Mt. Chabenec run approximately parallel to contours and range from 300-600 m long. We numbered the most prominent scarps 1 (downslope) through 8 (upslope) and studied scarps 2, 4, 6, and 7 (Fig. 3), which have lengths of 600 m, 350 m, 300 m, and 300 m, respectively. The vertical surface offset of the hillslope across these major scarps varies from about 1 m to as much as 10 m (Fig. 4). Scarps 1-8 all lie downslope of an arcuate downslope-facing scarp (Scarp 9). Scarp 9 appears to be the head of a detached slab that contains all the antislope scarps. Scarp 9 can be traced easily down the west flank of Chabenec's south ridge to about Scarp 6. Between Scarps 6 and 4 the scarp becomes a faint vegetation lineament; below Scarp 4 it projects to a gully that appears structurally controlled. If Scarp 9 defines the western edge of the slab that slid downslope and gave rise to the antislope scarps, the slab may be significantly thinner than inferred by Mahr (1977). For example, Scarp 9 outcrops only 55 m below the ridge

nose at Scarp 8, 65 m below the nose at Scarp 7, and 80 m below the nose at Scarp 6. If the slab has a planar bottom, then it is much thinner than the deep-seated gravitational slope deformation (DSGSD) mass inferred by Mahr (1977), which was inferred to be 135 m, 210 m, and 280 m thick at those same locations. If the slab is spoon-shaped then its thickness would be somewhat greater along its axis than at the edges. For example, given that the slab is only 600 m wide at Scarp 6, for its bottom to be 200 m deeper along its axis than at its edges only 300 m away would require the failure plane to be very deeply spoon-shaped in cross-section, sloping toward the axis at an average angle of 34°. An angle that steep would be more consistent with a wedge failure than with a slab failure.

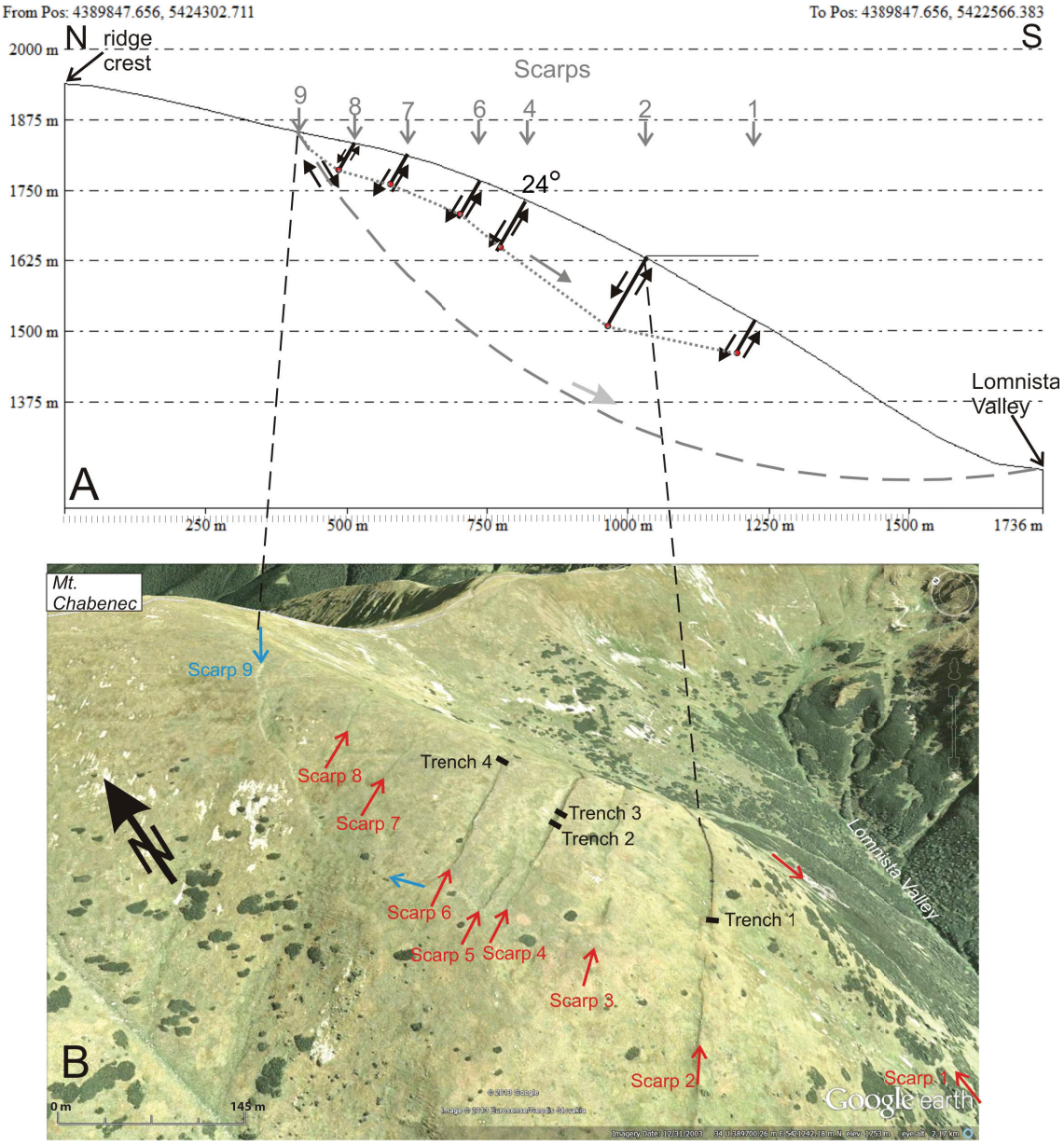

Fig. 3. Profile views of the southern slope of Mt. Chabenec. A – north-south topographic profile from the 30 m DEM (Shuttle Radar Topography Mission) that passes through scarps 1-9. No vertical exaggeration. The slope angle at Scarp 4 is 24°. The deep circular failure plane (dashed gray line, radius=1,250 m) is that of Mahr, 1977 (see Discussion). The gray dotted line shows the elevation of Scarp 9 as it descends the west flank of the ridge, which forms a minimum depth estimate for the failed slab. B – oblique view from Google Earth (satellite imagery draped over the DEM) looking slightly north of east, showing antislope scarps 1-8, downslope-facing scarp 9, and the locations of our four trenches.

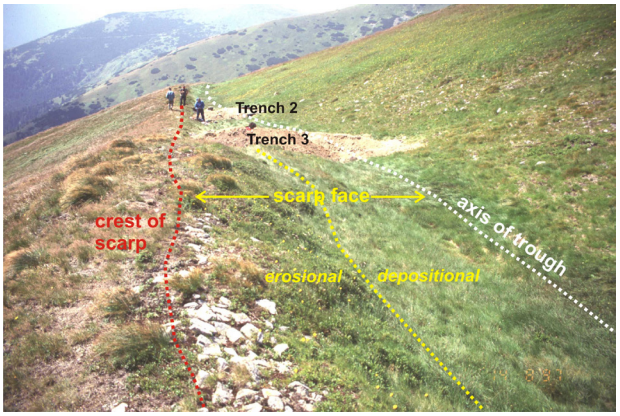

Fig. 4a. Photograph of the geomorphic components of a typical antislope scarp and its adjacent trough (Scarp 4, looking west). The slope uphill of the trough is mantled with normal residuum and colluvium, the latter of which is subject to downslope creep and slopewash erosion. Trenches 2 and 3 are visible in the middle ground; note people at Trench 2 for scale.

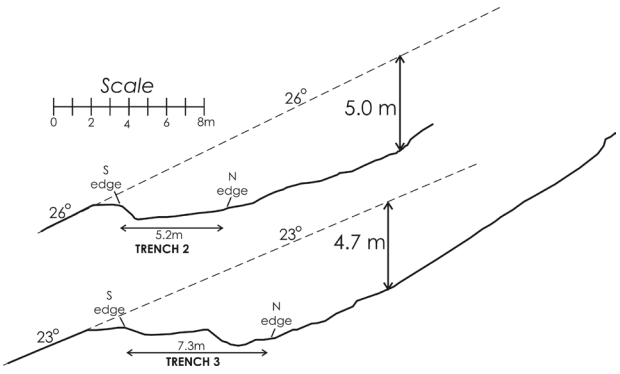

Fig. 4b. Topographic profiles across Scarp 4 at the locations of trenches 2 and 3. Dashed lines show the projection of the lower slope across the trough. Vertical surface offset across the antislope scarp ranges from 4.7-5.0 m, but is somewhat dependent on the slope angle projected and on exactly where the vertical offset is measured along the slope profile.

Trench 1 on Scarp 2

Scarp 2 is the longest (600 m) and tallest scarp at Mt. Chabenec (Figs. 3, 5). West of Trench 1 the trough has a low gradient to the west, with a near-horizontal depression at Trench 1. However, east of Trench 1 the scarp ascends diagonally upslope so the trough has a considerable westward gradient. Despite this gradient and the large slo-

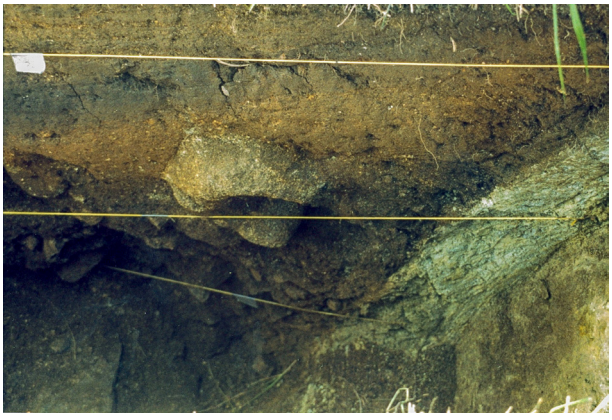

Fig. 5. Photographs of Scarp 2 and Trench 1. *Above*, looking west down the scarp. Trench 1 is at center. Note persons at center standing above and below the scarp. *Above right*, close-up of the east wall of Trench 1 where it cuts into the scarp face. Note the steep angle of the scarp face. *Below right*, view of main fault zone on the east wall. String lines are 50 cm apart. Light area at right is the granodiorite footwall of the main fault. Overlying it is a 20-30 cm-thick shear zone of decomposed granodiorite and grayish-green, clayey fault gouge (units 2a and 2b on the trench log, Fig. 6). The shear zone dips 57°N.

pe area that drains to the trough, there is no sign of erosion or channel development in the axis of the trough. We interpret this to mean that the scarp 4 is fairly young.

The scarp face is mantled with a tundra-like mat of turf grass, the top of which slopes 60°-70°N at Trench 1. This slope angle is well above the angle of repose for unconsolidated deposits, so prior to trenching we assumed the grass was growing on a bedrock fault plane. However, no bedrock was exposed anywhere on the scarp face. Trenching later showed that the grass is growing on a fine-grained sag pond deposit that had been tilted up to 50° by drag on the fault.

Stratigraphy and Soils

On the east trench wall we define 9 major units which were further subdivided into 18 subunits (Fig. 6). Unit 1 is the non-weathered granodiorite of the main fault footwall, and units 2a and 2b are decomposed granodiorite and fault gouge in the main shear zone, respectively. The oldest unconsolidated deposit (unit 3a) appears in the fault zone as a fault-bounded sliver. It is a yellow-brown silty clay interpreted as a sag-pond deposit from a closed depression. Later faulting dragged part of the deposit upward into the fault zone from some stratigraphic position beneath the trench floor. The remainder of the unconsolidated deposits and soils (units 3b through Oi) form a vertical sequence of subhorizontal strata. Unit 3b is the oldest layer in this sequence and is a gravelly silty sand, and appears to be a coarser channel deposit related to unit 3a. Unconformably overlying unit 3b are a sequence of much coarser deposits (4a, 4b) containing angular clasts of fresh granodiorite. Clast long axes plunge away from the fault, suggesting they were deposited as colluvium shed from a bedrock free face. In the northern part of the trench a correlative unit (4c) has a similar texture. Units 4a and 4b are overlain by unit 5B, the most laterally extensive deposit in the trough. This unit is red-brown sandy clay interpreted as a soil textural B-horizon developed in a sag pond deposit. The B-horizon is overlain by an A-horizon (unit 6Ab1; black silt). The sequence 4a-4b-5B-6Ab1 appears to be a single fining-upward sequence ranging from a basal colluvium to fine sag pond deposits, then topped by a well-developed soil profile; it comprises 1.0 m of the 1.5 m-thick trough deposits exposed in the trench. The soil is unconformably overlain by unit 7, a brown silty sand with some gravel that we interpret as a channel deposited in the trough axis. Unit 7 is overlain by a thin organic soil composed of an A-horizon (unit Oa) and either a peat layer in the graben (unit Oc) or a grass mat on the scarp face (unit Oi).

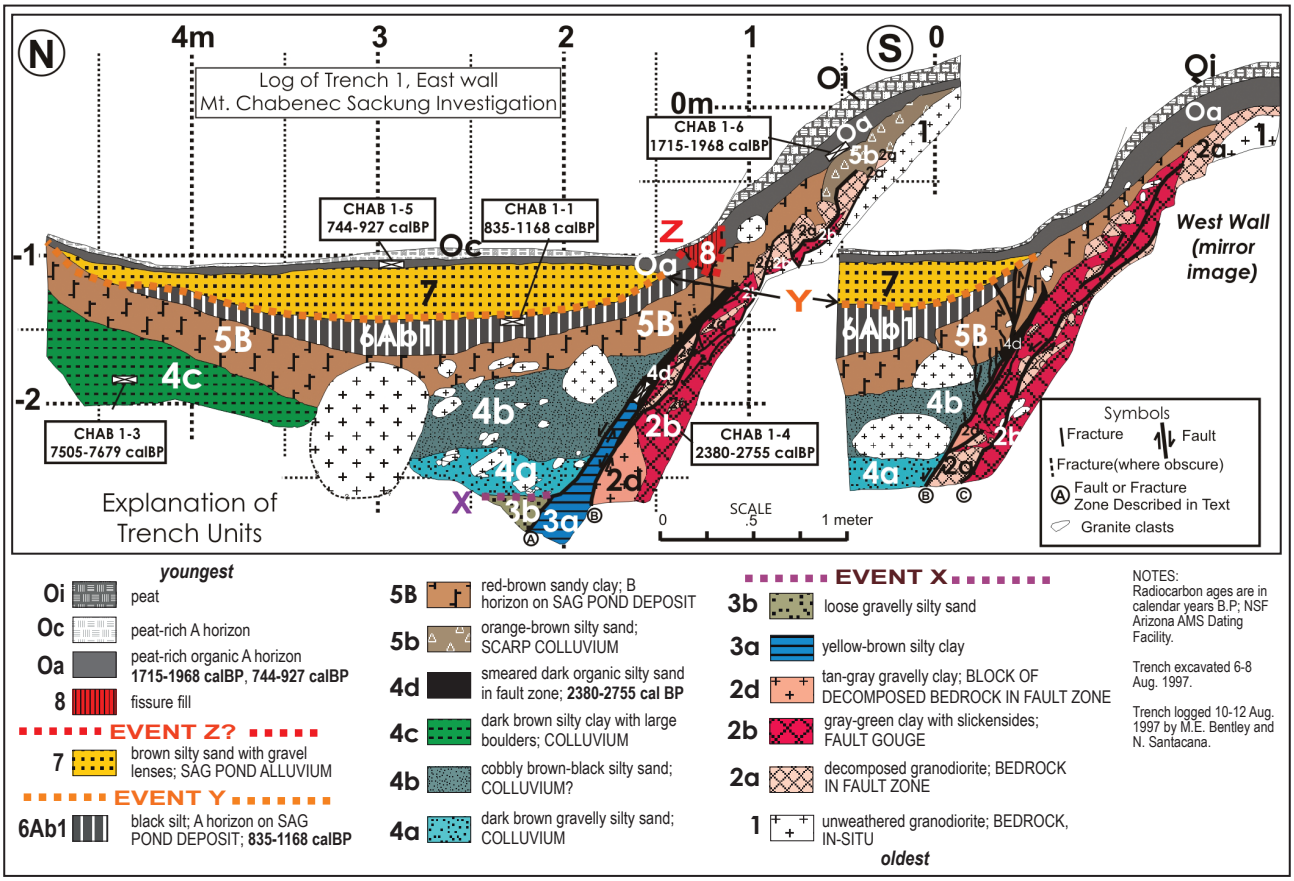

Fig. 6. Log of the east wall of Trench 1 (center and left) and a mirror image of the log of the west wall (at right).

Structure

The trench exposes only a single fault zone, a 25 cm thick bedrock shear zone that lies beneath the scarp face and extends to the bottom of the trench. The zone as a whole, and the individual fault planes within it, dip 55°-60°N. The fault footwall is composed of non-weathered granodiorite. The shear zone is composed of fault- and fracture bounded blocks of two materials: (1) decomposed granodiorite, and (2) grayish-green clay containing slickensides (fault gouge). There are two major fault planes within the shear zone, one centered in the 25 cm-thick zone, and another at the northern boundary of the shear zone. The fault in the center is undulatory with a wavelength of 0.5-1 m and an amplitude of ~10 cm. The northern boundary fault is straighter. On the east wall the northern fault bounds a sliver of hanging wall unit 3a, an old sag pond silty clay. On the west wall the northern fault contains at least 8 short faults that splay off at steeper dips and displace hanging wall deposits. The highest of these splay faults also appears on the east wall, where it underlies the fissure filled with unit 8. This splay fault contains the only evidence for most recent displacement event (Event Z on Fig. 6). On the west trench wall the splay fault displaces units 5B and 6Ab1, but not unit 7 or soil horizon Oa. On the east wall the splay fault also displaces units 5B and 6Ab1, but the overlying fissure disrupts soil horizon Oa. However, there is no net vertical offset of horizon Oa across the fissure, so it looks like a block of soil may have been plucked out of Oa, possibly by man-made action.

The structural relationships of the trough deposits/soils (listed from oldest to youngest) can be summarized as follows:

– unit 3a is a fault sliver within the main fault zone, dragged upward from a stratigraphic level beneath the trench floor;

Tab 1.
Radiocarbon ages from trenches on Mt. Chabenec. Sample locations are shown on the trench logs (Figs. 6, 8, 10, and 12).

Trench No.	Sample No.	Lab No.[1]	Material	^{14}C Age (yr BP, 1 sigma)	Calendar Age (cal yr BP) intercept(s) in parentheses, 2 sigma range[2]
1	1	AA27851	Organic silt	1,065±45	835 (960) 1,168
1	3	AA27852	Silty clay	6,735±55	7,505 (7,540) 7,679
1	4	AA27853	Organic silt	2,530±60	2,380 (2,720) 2,755
1	5	AA27854	Organic silt	925±45	744 (830) 927
1	6	AA27855	Peaty silt	1,905±50	1,715 (1,860) 1,968
2	1	AA27856	Charcoal in black mud matrix of angular gravel[3]	485±50	335 (520) 640
2	3	AA27857	Organic silt	1,170±45	970 (1,060) 1,229
2	4	AA27858	Organic silt	4,215±55	4,577 (4,740) 4,864
2	5	AA27859	Organic silt	1,825±45	1,625 (1,720) 1,870
2	6	AA27860	Organic silt	467±50	331 (510) 631
2	8	AA27861	Mud coatings in black-stained gravel[3]	4,965±55	5,594 (5,670, 5,690, 5,710) 5,890
2	9	AA27862	Smeared black organic silt in *shear zone*[4]	3,320±50	3,446 (3,490, 3,510, 3,550) 3,690
3	1	AA27863	Organic silt	1,880±45	1,711 (1,820) 1,924
3	2	AA27864	Detrital charcoal in sandy channel deposit	8,485±90	9,280 (9,450) 9,662
3	3	AA27865	Charcoal in organic clay smeared in shear zone[4]	2,640±75	2,491 (2,750) 2,945
3	4	AA27866	Detrital charcoal in gravelly channel deposit[5]	8,230±90	9,010 (9,210) 9,434
4	1	AA27867	Detrital charcoal in gravelly channel deposit	7,600±140	8,049 (8,370) 8,725
4	3	AA27868	Organic silt	1,565±55	1,343 (1,410) 1,563
4	5	AA27869	Organic silt	1,225±50	1,009 (1,160) 1,279
4	6	AA27870	Organic silt	945±50	742 (840) 937

[1] All analyses were made at the NSF Arizona AMS Facility at the University of Arizona, Tucson.

[2] Calendar-year Calibration from OxCal 4.3 (2017), using the IntCal13 calibration data set; Reimer et al., 2013.

[3] Radiocarbon- & calendar-age is considered to be younger than the true age of the deposit, because the dated carbonaceous coatings on gravel clasts may have been transported downward by infiltrating water from higher, younger deposits.

[4] Radiocarbon samples from the main shear zone may include carbon from more than one stratigraphic unit that was dragged up and smeared along the shear zone. Thus, the radiocarbon age does not necessary date the age of a faulting event, but the weighted average age of the carbon-bearing deposits dragged up in the fault zone.

[5] Radiocarbon samples from scarp-derived colluvial wedges may contain significant carbon derived from the erosion of older deposits exposed in the scarp free face. In this case, the sample's radiocarbon age will not date the deposition of the colluvial wedge, but rather the age of carbon in the deposit exposed in the free face, which could be much older than the wedge.

– units 3b through 4b are in fault contact with the shear zone;
– units 5B and 6Ab1 are dragged upward onto the scarp face and faulted by the splay fault beneath the toe of the scarp;
– unit 7 is undeformed (i.e., post-dates sackungen movement).

The Petrography Laboratory at SGIDS described the shear zone material as follows:

"Clay gouge… distinct slickensides sloping to the North. The common accompanying features of these tectonic planes were well-developed mylonite zones with tectonic gouges. Tectonic gouges in the faults are known from civil engineering practice from various sites throughout Slovakia. ... with clayey fillings of fault zones consisting of illite-montmorillonite, with less kaolinite, palygorskite-sepiolite and carbonates….petrographical analysis of the tectonic gouge from the Chabenec site defined argillitized and weathered granodiorite. In the separated clayey fraction Dr. Žáková from SGIDS identified in 2001 the presence of illite and quartz, with admixture of highly dispersed feldspars using Roentgen Diffraction Analysis." Analytical data are reported in Appendix 1.

Geochronology

In the graben, the surface soil (unit Oa) dates at 744–927 cal BP and the underlying buried soil (6Ab1) dates slightly older at 835 to 1,168 cal BP (Table 1). However, horizon Oa on the scarp face dates older than either of the above ages at 1,715 to 1,968 cal BP, which presents a contradiction. Note that on the east wall horizons Oa and 6Ab1 merge at the toe of the scarp. This suggests that the A-horizon organic material (peat) on the scarp face must be time-equivalent to both A-horizons in the graben. That is, the scarp face A-horizon continued to develop and accumulate carbon during the deposition of multiple soils and deposits in the graben. The scarp-face soil would thus be a relict soil. The fact that the scarp face Oa sample yielded an age even older than 6Ab1 indicates it contains a mixture of even older carbon. Where could such older carbon have come from? One possible source is from older Holocene units deposited in the trough, which were then dragged up onto the footwall by faulting, and then eroded/redeposited on the scarp face directly beneath Oa, in a unit such as 5b. We know that carbon-bearing sediments have been dragged up the fault zone in the past because fault sliver 3a, dragged at least 1 m upward, contains carbon dated at 2,380 to 2,755 cal BP, which is even older than the age from scarp face Oa.

Interpretation

Based on stratigraphic superposition, cross-cutting relationships, and the occurrence of two paleosols, we interpret a sequence of at least three (possibly four) Holocene deformation events at Trench 1, with two more questionable events (Table 2). Age control for deformation events comes from radiocarbon dates of sediments deposited in structural depressions (Table 1). This approach to dating deformation events derives from paleoseismic studies of normal faults (e.g. McCalpin, 2009, Chapter 3).

Tab. 2.
Inferred sequence of depositional, pedogenic, and deformational events affecting Trench 1.

Event (oldest at bottom)	Evidence
8-Deformation EVENT Z?	A fracture forms at the scarp toe in soil horizon Oa and fills with fissure-fill unit 8. The fracture correlates with a similar splay fault on the west trench wall; however, there is no corresponding fissure on that wall. The fissure may possibly result from some human or animal disturbance, which plucked a root ball out of the ground.
7-Develop soil horizons Oa and Oi	Weak modern soil develops on unit 7 alluvium, with a possible loess component. Base of Oa horizon on scarp face **1,715 to 1,968 cal BP;** horizon Oa in graben, **744 to 927 cal BP**.
6-Deposit unit 7	Unit 7 deposited as alluvium in the newly-deepened trough.
5-Deformation EVENT Y	Unit 3a is faulted against units 3b, 4a, 4b; Units 5B and 6Ab1 are faulted and dragged up onto scarp face. Trough deepens by ~0.5 m.
4-Deposit units 4-5-6	Scarp-derived colluvium (units 4a, 4b) deposited from the south. Coeval slope colluvium (unit 4c) deposited from the north (**7,505 to 7,679 cal BP**). Over a long time, silt (aeolian?) washed into the trough, depositing unit 5 which fills in a broad trough. Soil horizons 5B and 6Ab1 then form (**soil top, 835 to 1,168 cal BP**).
3-Deformation EVENT X	Trough deepens due to faulting.
2-Deposit units 3a, 3b	Yellow-brown silty clay accumulates in standing water in a closed depression (unit 3a; **2,380 to 2,755 cal BP**). Later streamflow brings coarser alluvium into depression (unit 3b). Unit 3a now preserved only in a fault-bounded sliver.
1-Deformation EVENT W	Normal faulting creates the initial topographic trough.

Scarp 4 (Trenches 2 and 3)

Scarp 4 is 350 long with a vertical surface offset of ~5 m (Fig. 4). Scarp 4 is nearly parallel to contours, so the trough axis has a low gradient (Fig. 3). East of the trench site the scarp crest is composed of granodiorite of the sackungen footwall (Fig. 7, left). Elsewhere the scarp face is mantled with a tundra-like mat of turf grass, which slopes N at greater than 35°-45°. We located Trenches 2 and 3 in the center of the scarp where the trough axis was nearly horizontal (Fig. 9). The scarp here was relatively low (vertical surface offset of 4.7-5 m), the trough axis was horizontal, the trough was a recent depocenter, and thus the lower part of the scarp had been buried by recent sedimentation (Fig. 7, right). We inferred that this site would have a thick record of post-sackungen sedimentation. Farther east (Fig. 7, left) the trough axis had a steeper gradient, was more erosional than depositional, so the scarp was accordingly higher and steeper. Although the scarp was more impressive there, we inferred it would have thinner or less complete records of trough sedimentation, making it less suitable for trenching.

A second feature of the trench site was complexity of the scarps. As shown in Fig. 7-right the trough contained a secondary scarp (Scarp 4B) parallel to the main scarp. At Trench 3 Scarp 4B is the higher of the two, but it becomes smaller westward and dies out between Trenches 2 and 3. The modern drainage follows the base of the Scarp 4B, but once Scarp 4B dies out the channel turns 45° and southward to the base of Scarp 4A. We felt that having two parallel sackungen faults bounding an intermediate structural block would permit better differentiating of displacement events via cross-cutting relationships. So we excavated Trench 3 across both scarps and Trench 2 across the main scarp past where the secondary fault had died out at the surface. The secondary fault was also exposed in Trench 2.

Trench 2, Stratigraphy and Soils

On the east trench wall 14 major units were defined which were further subdivided into 44 subunits (Fig. 8). Units 1-3 are bedrock and shear zone units and will be described in the next section. The oldest unconsolidated deposits (units 4, 4a) are sandy and silty gravels that overlie weathered granodiorite bedrock (unit 3). Unit 4 is overlain by unit 5a, a well-sorted fine gravel that is clearly alluvial, so it may have been deposited by runoff in the sackungen trough after trough formation (5,594 to 5,890 cal BP). It is unclear if the unit 4-4a gravel is a trough alluvium (post-dates trough creation) or a slope colluvium that predates trough formation.

The log shows the former interpretation (i.e., the Event X horizon underlies units 4 and 4a). Units 6, 7, and 8 are well-sorted fine gravels interpreted as trough alluvium. On both sides of the main fault zone unit 8 is overlain by a lens-shaped body of colluvium (units 9a, 9b) which we interpret as scarp-derived colluvial wedges. Unit 10 is a 0.8 m-thick stack of talus deposits, solifluction deposits, and colluvium. The upper subunits (10d, 10e) thin toward the scarp, suggesting that they (and perhaps the rest of unit 10) were derived from the hillslope upslope of the trough. Unit 10 is overlain by a significant change in the type and pattern of sedimentation, to that of fine-grained (sag pond) deposits in the trough (units 11a, 11b, 12a) and small wedges of scarp-derived colluvium (unit 11c) on the trough margins. This rapid change suggests reactivated displacement on the sackungen scarp and deepening of the trough. Overlying unit 12 is unit 13 (composed of massive silts interpreted as loess) and well-sorted sands and fine gravels

Fig. 7. Left – photograph of Scarp 4 about 50 m east of Trenches 2 and 3 (visible at far right center). Note outcrops of granodiorite along the scarp crest (center to left edge). Right – photograph of Scarp 4 looking southwest, with Trench 3 (7.3 m long) at left and Trench 2 (5.2 m long) at right. Trenches are 21 m apart. A group of trench diggers sits/stands on Block I. Lomnistá Valley in background.

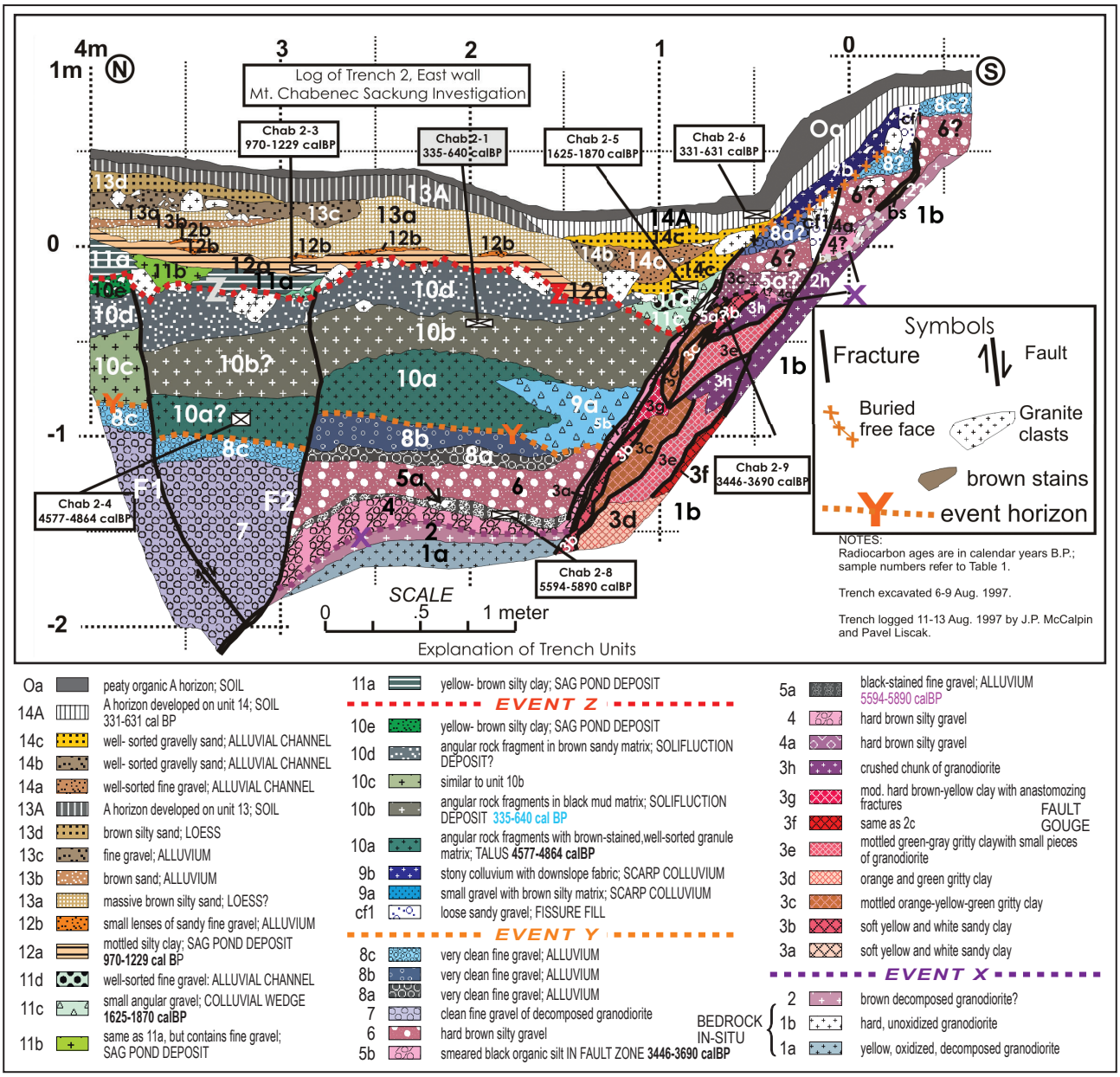

Fig. 8. Log of Trench 2. Three displacements events (from youngest to oldest, Events Z, Y, and X) are interpreted from colluvial wedges, upward fault terminations, and abrupt changes in sedimentology (see text for details). The graben structure at left does not reach the ground surface and has no topographic expression; it is probably the subsurface continuation of the fault beneath Scarp 4B (exposed in Trench 3).

(alluvium). A soil A-horizon then developed on unit 13 (unit 13A). At the foot of the scarp units 13a and 13A have been eroded out by a younger channel containing units 14a-b-c. A younger A-horizon (unit 14A) then developed on unit 14, followed by the formation of a peaty organic soil horizon (unit Oa) over the entire scarp and trough.

Trench 2, Structure

The trench exposes two fault zones. The main fault zone is a 50 cm-thick shear zone in bedrock that lies beneath the Scarp 4A face and dips 55°-60°N, and is exposed down ~1.5 m to the floor of the trench. The fault footwall is composed of granodiorite fractured by four joint sets (Fig. 9, left). Set 1 strikes perpendicular to the trench with fractures spaced 15-30 cm apart. Set 2 strikes parallel to the trench on a10-15 cm spacing. Sets 3 and 4 form a 30°/60° conjugate pattern on the plane of the footwall. The four joint sets break the footwall granodiorite into angular blocks 5-10 cm in diameter. There is oxidation along all joints but it does not penetrate the center of the joint-bounded blocks.

Fig. 9. Photographs of the main fault zone in Tench 2. Left – fractured granodiorite of the fault footwall at lower right. Shear zone is visible below lower string line. Right – closeup of shear zone. String lines are 50 cm apart.

The 50 cm-thick shear zone contains 5 to 6 discrete fault planes (Fig. 8). The outermost fault planes are long and relatively planar whereas the inner faults have a more anastomosing or en-echelon pattern. This pattern creates numerous fault-bounded slivers and lenses of contrasting color and texture (units 2a through 2h; see Fig. 12, right). All subunits are basically fault gouge with textures ranging from clay to sandy clay to gritty clay, and colors ranging from white, yellow, yellow-brown, orange, and green. The coarsest units (2c, 2e) contain visible angular pieces of unweathered granodiorite within the clay matrix, presumably ripped off the footwall and rolled into the gouge during rapid slip events. The northern margin fault has dragged up and smeared a thin layer of black organic silt into the fault zone (unit 5b). This disturbed layer appears to be derived from unit 5a and perhaps unit 4 in the trough sequence. The main shear zone does not extend to the ground surface, but is overlain on the upthrown side by a series of unconsolidated deposits. These beds resemble units 5a, 6, and 8a/8c on the downthrown side of the fault. If this correlation is correct, we can measure a vertical displacement of 2.0 m across the shear zone, based on the net offset of the base of unit 6. Faults in the shear zone displace units as young as 11d but do not displace unit 14.

A second fault zone is exposed 1.5 m north of the main shear zone, beneath the sackungen trough, composed of two subvertical faults (F1, F2) with a downdropped block between them. Fault F1 terminates into F2, indicating that F2 is the master fault. F2 also has evidence of greater vertical displacement, since it drops bedrock (units 1a, 3) and the older alluvial units (4, 5a, 6) down below the floor of the trench. The fault juxtaposes these units against a thick unit 7, which has no counterpart south of the fault. Higher on the F2 fault plane units 8 and 10 exist on both sides of the fault and are displaced about 10 cm down-to-the-north. From these relationships we can infer that: (1) F2 forms the northern margin of a structural block floored by bedrock, (2) F2 had large vertical displacement of units 1a through 6 prior to the deposition of unit 8, and (3) since deposition of unit 8 there has only been a minor 10 cm of reactivated movement on F2. The net vertical displacement across F1 and F2 since unit 8 time is negligible, indicating the faults mainly accommodate a small amount of horizontal extension. Faults F1 and F2 displace units as young as 10e, but are overlain by units 11a and younger.

Trench 2, Geochronology

Trench 2 yielded seven radiocarbon dates, the most from four trenches. Overall the dates indicate that trough sedimentation on the structural block began prior to 5.7 ka (unit 5a) and continued episodically through the latest Holocene. However, units 5a and 10a are matrix-free fine gravels where all the clasts are stained black or brown, and it is this stain (actually thin silt films on talus clasts) which was dated. It is not clear whether the black stains are primary depositional features, or younger illuviated components deposited by organic-rich groundwater. In other trenches, radiocarbon dates from these black-stained gravels have yielded anomalous ages compared to dates from less porous/ permeable deposits. A second problem with the dates in Trench 2 is age reversals. For example, unit 10b yielded an abnormally young age (335-640 cal BP) compared to older ages from higher units. In fact, the date from unit 10b is nearly identical to that from the surface soil 14A (331 to 631 cal BP). The most likely explanation for this correspondence is that the carbon sampled in unit 10b was contaminated with intrusive carbon from unit 14A. The third-oldest date from the trench (3,446 to 3,690 cal BP) came from unit 5b in the shear zone. As

in Trench 1, it is difficult to interpret this date, given the opportunities for physical mixing of carbon-bearing materials in the shear zone. The texture of unit 5b and its physical continuity with unit 5a near the bottom of the trench indicate it is mostly derived from units 4 and 5a. But unit 5b dates 2,200 years younger than in-situ unit 5a. To attain its present high position in the shear zone, the dated sample from unit 5b had to be dragged up the fault past units 6 through 10b. Notably, unit 10b contains very young carbon (as described above), so that is one possible source for mixing younger carbon into unit 5b.

Trench 2, Interpretation

We interpret a sequence of at least three (possibly four) Holocene deformation events at Trench 2 (Table 3). Age control comes from seven radiocarbon dates from sediments exposed in the trench walls (Table 1).

If this correlation of units 6-8 across the shear zone is correct, it implies that prior to deposition of unit 5a, erosion had removed all scarp relief at this site, as it has in the modern landscape where large swales cross the antislope scarps. Local alluviation then overfilled the trough and entirely buried the antislope scarp during unit 5-8 time. Later, during deformation Events Y and Z, the main fault reactivated, dropping units 5-8 two meters down in the trough.

Trench 3, Stratigraphy and Soils

On the east trench wall we define 14 major units which were further subdivided into 33 subunits (Fig. 10).

Units 1-3 are bedrock and shear zone units and will be described in the next section. The oldest unconsolidated deposits (unit 4a, 4b) are gravelly sand and silty sand that overlie weathered granodiorite bedrock (unit 2).Unit 4b is interpreted as a sag pond deposit, indicating it was deposited in an early sackungen depression. The overlying unit 5 coarsens upward, from gravelly sand (unit 5a, colluvium) to unit 5b (talus). Unit 5 is unconformably overlain by unit 6, which has a small alluvial channel fill (unit 6a) at its base but is mostly composed of unit 6b, a gravelly sand (colluvium). Unit 6b is overlain by a 40-50 cm-thick lobe of compact silty sand full of angular rock fragments (unit 7). Because this unit pinches out toward the Scarp 4A and contains rock fragments typical of the slope above the trough, we interpret it as a solifluction lobe. Overlying unit 7 near scarp 4A is unit 8, a finer alluvium that hosts three soil horizons (A, AB, and B). The B-horizon contains the most pedogenic development as judged by color (red-brown) and clay content, qualifying as a textural B-horizon. Unit 8 thins northward away from Scarp 4A. This geometry may reflect the original deposit shape, as a channel fill deposited against the scarp. Or it may re-

Tab. 3.
Inferred sequence of depositional, pedogenic, and deformational events affecting Trench 2.

Event (oldest at bottom)	Evidence
8-Erode channel at toe of scarp and deposit unit 14	Streamflow down trough axis erodes a 0.4 m-deep channel at toe of scarp, followed by deposition of alluvial gravel and sand (units 14a-b-c). Soil 14A develops on unit 14 (**331 to 631 cal BP**). Later the entire trough floor is covered by a peaty organic A-horizon (unit Oa).
7-Deposit units 12a-13d	A thin sag pond deposit (12a; **970 to 1,229 cal BP**) is laid down over the whole trough floor, followed by thin alluviums (12b, 13b-13c) and two loesses (13a, 13d). A soil A-horizon forms on unit 13 (13A).
6-Deposit units 11a-11d	Unit 11c is a scarp-derived colluvial wedge (**1,625 to 1,870 cal BP**). Coeval trough axis facies (sag pond deposits 11a, 11b) are deposited.
5-Deformation EVENT Z	Units 1a through 8c? faulted on main shear zone ~1.2 m.
5-Deposit units 10c-10e	Continued alluviation in trough.
4-Deposit unit 9a	Scarp-derived colluvium (unit 9a) deposited in trough; possibly coeval colluvium 9b deposited on scarp face. Coeval alluvium (unit 10a) deposited in trench axis **(4,577 to 4,864 cal BP)**.
3-Deformation EVENT Y	Displacement on main shear zone of ~0.8 m.
2-Deposit units 5a through 8b	Alluvial units 5a **(5,594 to 5,890 cal BP)** through 8b are deposited in the sackungen trough.
1-Deformation EVENT X	Normal faulting creates the initial topographic trough; main fault displaces units 1 (bedrock) and possibly 4 (if it is the pre-faulting colluvium on the slope).

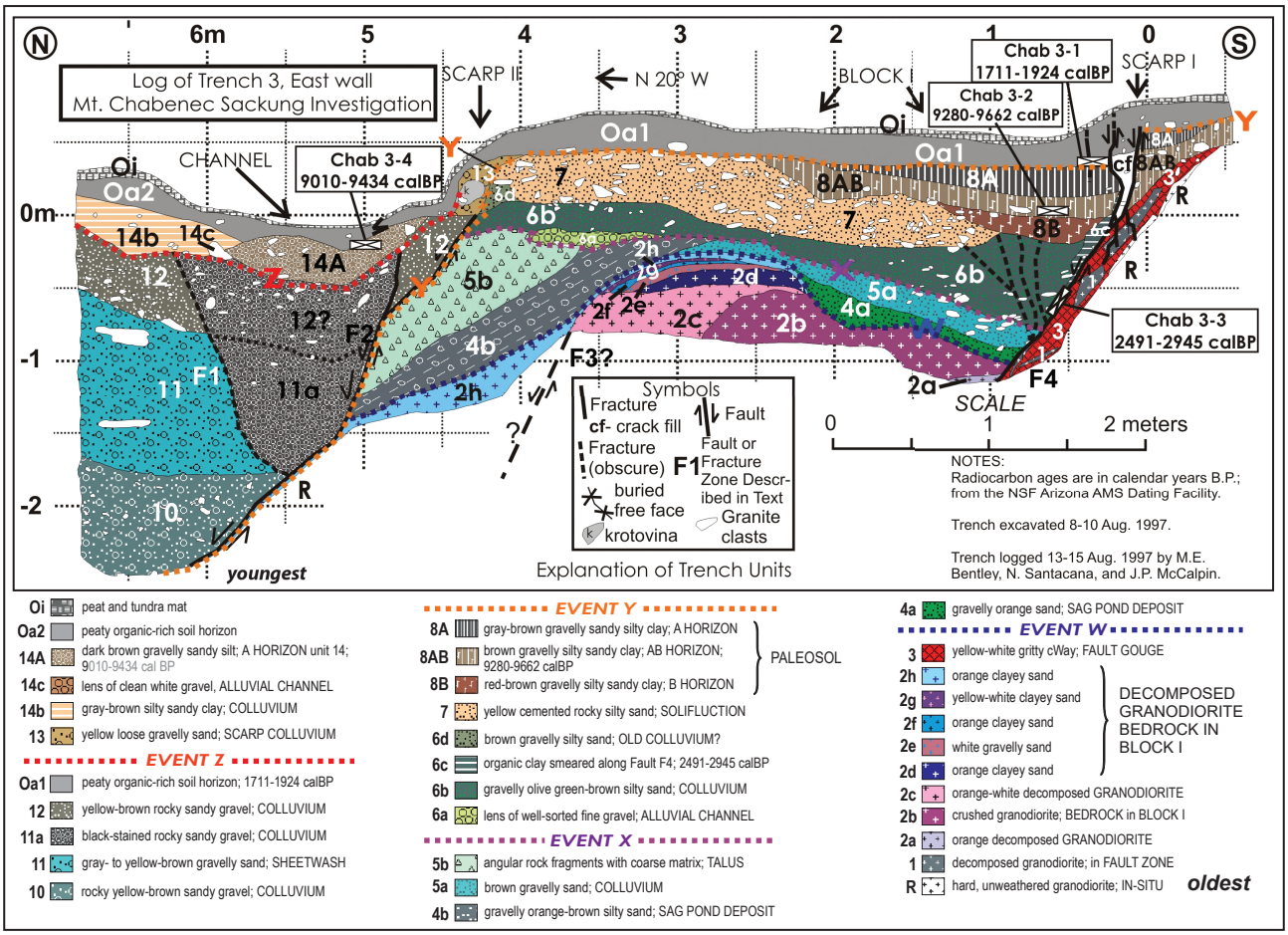

Fig. 10. Log of the east wall of Trench 3.

present erosion of a more laterally-extensive deposit that was tilted up-to-the-north by block faulting. Both units 7 and 8 are capped by a peaty, organic soil A-horizon (unit Oa1) that contains very rare clasts. This unit parallels the modern ground surface so is in angular unconformity with underlying tilted units 7 and 8. However, the horizon thins drastically as it goes over the face of Scarp 4B, as if it were stretched by faulting.

None of the trough deposits described above exist north of Scarp 4B and fault F2. Instead, the northern trough is underlain by much thicker, massive gravel deposits. Unit 10 is sandy gravel interpreted as colluvium, while unit 11 is finer (gravelly sand) interpreted as a slopewash deposit. Unit 12 is a yellow-brown rocky sandy gravel interpreted as colluvium sourced from the north. Between faults F1 and F2 all clasts in units 11 and 12 have been stained black. We infer this is some type of groundwater staining mechanism. Unit 12 is unconformably overlain by a clayey sag pond deposit (unit 14b), a small gravel channel (unit 14c), and an A-horizon developed on younger sandy silt (unit 14A). Unit 14 is overlain by peaty soil horizon Oa2, a thinner and younger version of unit Oa1.

In Trench 3, the Quaternary strata on Block 1 (units 4 through 8) represent only the early record of deposition in the trough, prior to the development of Scarp 4B. These four units comprise a 1.1 m-thick sequence of older trough sediments that overlie crystalline bedrock, and which correlate with the older half of the trough fill exposed in Trench 2 (units 4 through 10a, also ~1 m thick). After uplift of Block I in the mid-Holocene, trough deposition at Trench 3 shifted to the north of Block I and Scarp 4B, and units 10-14 were deposited. The correlative beds in Trench 2 are units 10b-14A, which comprise the upper half of Quaternary deposits there.

4.3.6 Trench 3, Structure

Based on the sharpness of scarps at the surface (Scarp 4B younger than Scarp 4A), and on cross-cutting relationships in the trench wall, fault movement has generally progressed in time from the main shear zone (F4), to faults F3, then F2 and F1. For example, the oldest trough fill (unit 4a) lies against the main shear zone (F4), indicating that movement on F4 created the initial trough.

Those thin units (4a, 5a) are no longer horizontal but are backtilted strongly toward F4, which requires movement on another normal fault farther north (F3). Movement on F3 is also required to drag/tilt units 2h-4b-5b down-to-the-north. These tilted strata are truncated by F2; slip on F2 is also required to tilt units 6-7-8 down-to-the-south. So the progression of movement from F4 to F3 to F2 is well documented by cross-cutting. Fault F1 appears to be the youngest structure, being an antithetic fracture growing upward from F2 which has not yet accumulated significant vertical displacement.

Trench 3, Geochronology

At first glance the radiocarbon ages from Trench 3 seem too old and too inconsistent compared to those in nearby Trench 2. Two samples very close to the modern ground surface yielded anomalously old early Holocene ages (Chab 3-4, only 10 cm below the surface, 9,010 to 9,434 cal BP; Chab 3-2, 25 cm below the surface, 9,280 to 9,662 cal BP). By comparison, sample Chab 3-1 (15 cm below the surface, and only 10 cm higher than Chab 3-2) yielded an age of 1,711 to 1,924 cal BP. This age is reasonable compared to ages from Trench 2. One reason for this inconsistency is that there has been no trough sedimentation on Block I since faulting Event X (see Fig. 10). Since Block I was abandoned by active deposition, a moderately strong soil profile (8A-AB-B-horizons) has formed, which has subsequently been tilted south and the north halves removed by erosion. The soil development alone suggests that unit 8AB (site of the 9.4 ka sample Chab 3-2) is probably at least early Holocene in age. However, this line of reasoning cannot explain the early Holocene age of sample Chab 3-4 (9.2 ka), which is not on Block I and overlies much younger trough deposits. Our tentative interpretation is that the carbon sampled in sample Chab 3-4 was partly derived from erosion of units 8A or 8AB when they were exposed in a free face of Scarp 4B. If sample Chab 3-4 contained an intact colluvial chunk or block of horizon 8A, which was then overprinted by younger A-horizon 14A, it might have been difficult for trench loggers to distinguish the two A-horizons. Notably, sample Chab 3-4's age (9,010 to 9,434 cal BP) overlaps the age of in-situ unit 8AB (9,280 to 9,662 cal BP) at two sigma, suggesting they are related.

The late Holocene age of carbon in the main shear zone (Chab 3-3, 2,491 to 2,945 cal BP) is also problematic. Recall that in Trench 2 a similar shear-zone sample (Chab 2-9) yielded an age of 3,446 to 3,690 cal BP. That age was midway between radiocarbon ages at the bottom (5.6 ka) and top (1-1.8 ka) of the trough stratigraphic sequence, and we speculated that older and younger carbon had been smeared along the fault zone and physically mixed, yielding an intermediate age. That argument cannot apply to the sample from the Trench 3 shear zone, because all possible source beds for smeared-upward carbon (units 4a, 5a, 6b) are older than ~9.5 ka, so smearing them together should never yield an age of ~2.7 ka. The only way to explain such a young age is to argue that younger carbon was somehow introduced into the shear zone from above, from sources such as the crack fill at the top of fault F4 (labeled "cf" on Fig. 13). That fissure displaces carbon-bearing units 8A and Oa1, and could possibly have opened deep enough along the fault plane to allow some

Tab. 4.
Inferred sequence of depositional, pedogenic, and deformational events affecting Trench 3.

Event (oldest at bottom)	Evidence
Deposit unit 14	Unit 14 deposited in closed depression. Downwarped soil Oa1 continues to develop and accumulate carbon, but is slightly eroded by the modern drainage channel.
Deformation EVENT Z	Small displacement on F4 displaces units 8A and 8AB 25 cm down-to-north. Larger displacement (~0.5 m) occurs on F2, displaces soil Oa1. This movement also tilts unit 13 to near-vertical. Brings Scarp 4B to its present height.
Deposit units 10-13	Unit 13 deposited as a small scarp-derived colluvial wedge. Thick units 10 through 12 are deposited in the new trough created by faults F1 and F2 (~2.5 m thick). Soil horizon Oa1 forms across surface (basal age of **1,711 to 1,924 cal BP**).
Deformation EVENT Y	Much larger displacement occurs on F2 displacing units 4b through 7 down-to-the-north below the trench floor (minimum of 2.8 m). Units 4a through 8A are tilted more down-to-south, to their present dip angle. Later erosion planes off the northern halves of 8AB and 8A.
Deposit unit 6-8	Units 6, 7, and 8 are deposited. A strong soil profile (A-AB-B-horizons) develops on unit 8. Base of unit 8AB dates at **9,280 to 9,662 cal BP**.
Deformation EVENT X	Fault F3 develops, creating Block I. Block I deposits between F3 and F4 are tilted down-to-south by domino-style normal faulting, to roughly half their present dip. Movement on F3 also tilts and downdrops units 4b and 5b.
Deposit units 4 and 5	Units 4a and 5a were deposited in trough at base of main shear zone, sourced from the south; coeval units 4b and 5b have different lithology, so presumably sourced from north.
Deformation EVENT W	Initial sackungen displacement occurs on main shear zone (F4).

Fig. 11. Photographs of Trench 4 on Scarp 6. Left – looking southeast with Scarp 6 in the middle ground and the unnamed NW-trending scarp coming in from the lower left corner. Trench 4 is behind the light-colored spoil pile. Right – Trench 4 looking southwest.

late Holocene carbon to infiltrate down to the depth of sample Chab 3-3. In summary, half of the four samples collected yielded ages that cannot be reconciled with the physical stratigraphy, and must be explained away by some complicated movement/intrusion of younger or older carbon.

Trench 3, Interpretation

Based on stratigraphic superposition, cross-cutting relationships, and the existence of a strong paleosol, we interpret a sequence of four deformation events at Trench 3, the latest three of which are Holocene (Table 4).

Scarp 6 and Trench 4

Scarp 6 is roughly 300 m long and lies about 90 m north of and parallel to Scarp 4. The ambient slope of the ridge at Trench 4 is gentler than at Trenches 1-3 farther downslope (Fig. 11, left). The Trench 4 site is somewhat unique because it was sited where Scarp 6 was intersected by another antislope scarp coming in from the NW. The intersection of the two antislope scarps created a triple-junction occupied by a closed depression. The scarp faces here are relatively low and gentle, mantled with a tundra-like mat of turf grass.

Trench 4, Stratigraphy and Soils

On the west trench wall we define 10 major units further subdivided into 22 subunits (Fig. 12).

Unit 1 is in-situ crystalline bedrock of the main fault footwall, and unit 2 is the oldest Quaternary deposit (a sag-pond silt) overlying bedrock. The silt is exposed only on the footwall and is unconformably overlain by a series of thick talus deposits (units 3a, 4a; 1.4 m thick) which dip 10°-15°S. This dip is similar to that of the slope gradient north of the trench, so we presume it is the original depositional dip. Similar thick talus units (4b, 4c, 4d; 1.4 m exposed thickness) exist on the hanging wall of the main fault. We tentatively correlate these talus units, acknowledging that: (1) the contact of talus (unit 4) over sag pond silt (unit 2) is not exposed on the hanging wall, (2) the stony character of unit 3a is not reproduced in units 4b or 4c, and (3) the 3a-4a contact is not recognized between hanging-wall units 4b-4d, possibly due to the black (groundwater) staining of unit 4c. The presence of thick talus on both sides of the main fault indicate that no sackungen scarp existed here when units 3 and 4 were deposited, even though a trough must have existed earlier (unit 2). Within the main shear zone, unit 3b appears to be a fault sliver derived from units 3a and 4a, whereas unit 4e appears to be a sliver derived from hanging wall units 4b-4d. Overlying unit 4 is a non-talus unit 5, interpreted as colluvium. Unit 5b abuts the main fault and has the shape of a colluvial wedge. Units 5c and 5d are fault slivers that share the texture of units 5a-5b and do not contain angular talus clasts, so are younger counterparts of fault slivers 4e and 3b. Unit 5a thins slightly away from the fault and does not exist on the footwall, thus appears to have been deposited only in a sackungen trough created by movement on the main fault zone.

The style of sedimentation changes after unit 5, to a series of thin trough channel and sag pond deposits. Units 6, 7a, and 7b were deposited in channels that flowed down the trough axis. Unit 7c is a scarp-derived colluvial wedge contemporaneous with unit 7b. Units 7b and 7c are overlain by sag pond silty clay (unit 8), indicating a closed depression. Deposits coarsen upward to unit 9, another channel deposit, upon which a modern soil horizon has developed (units 9A and 10).

Trench 4, Structure

Trench 4 exposes a series of about 12 north-dipping normal faults which we group into six fault groups. Faults F3 to F6 are individual faults in the main shear zone that

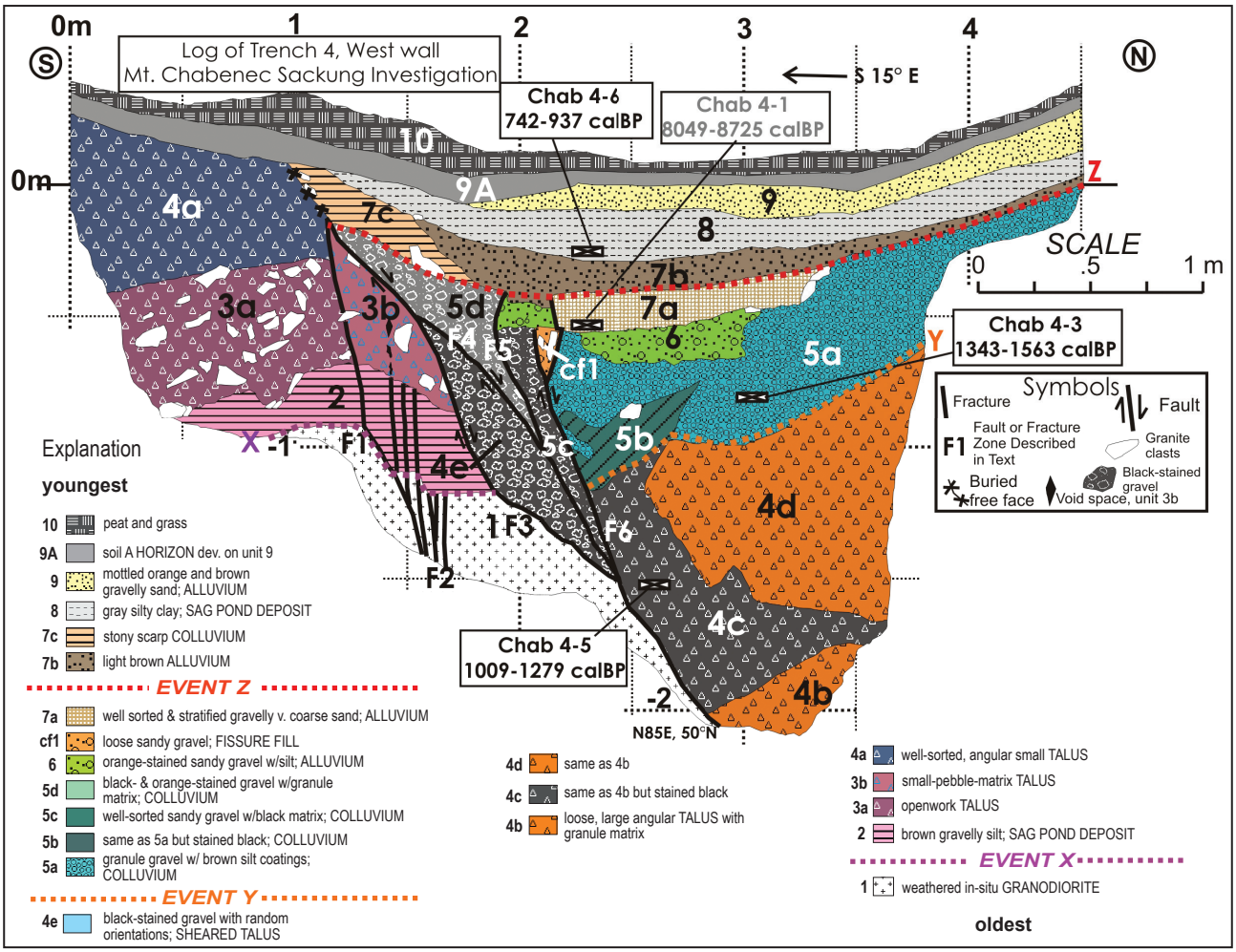

Fig. 12. Log of west wall of Trench 4.

underlies the surface scarp, whereas Faults F1 and F2 lie in the footwall of the main shear zone. On these faults we observe the same age progression of faulting as seen in other trenches. The earliest fault is not expressed in surface morphology, but must lie south of Trench 4, because even the upthrown side of the present scarp was a trough at that time (unit 2 deposition). Faults F1 and its secondary strands (F2) affect only the older units. For example, the three northern strands of F2 displace bedrock but not unit 2; the three southern strands displace unit 2 but not unit 3. F1 displaces units 2-4, but the total vertical displacement of unit 2 across F1 and F2 is only 30 cm.

Most of the displacement exposed in the trench has occurred on the main shear zone (faults F3 to F6). Faults F5 and F6 splay upward off Faults F3 and F4 and displace younger hanging-wall deposits. Units 6 and 7a are displaced by both F5 and F6, whereas unit 7b unconformably overlies both faults and is not displaced. This relationship, and the existence of scarp-derived colluvial wedge 7c, indicates the latest fault movement occurred after unit 7a but before unit 7b and 7c. An older event seems to be indicated by the fact that a fissure fill (unit cf1) was deposited near the top of fault F6, then was overlain by alluvial unit 6, after which unit 6 was faulted again.

Trench 4, Geochronology

Four radiocarbon samples were collected, two from the younger, well-stratified alluvial-sag pond section (units 7-8), and two from the older massive colluvium-talus deposits (units 4 and 5). The only age that appears reasonable, compared to those from other trenches, is that of the youngest sample (Chab 4-6 from sag pond unit 8), which dated at 742 to 937 cal BP. The next deepest sample (Chab 4-1) also comes from a thin stratified unit (alluvial unit 7a) but yields a much older age (8,049 to 8,725 cal BP). If this age was correct, then there would have to be a hiatus of 8,000 years between faulted unit 7a and unfaulted units 7b and 8. A comparable hiatus was exposed in Trench 3 (~7.7 ka), but there a well-developed soil profile consisting

of an A, AB, and textural B-horizon had developed during the hiatus, as expected. In contrast, in Trench 4 there is no soil development whatsoever in the faulted units (7a and older), which would be an unlikely occurrence in a 8 ka hiatus. Sample Chab 4-1 was one of three detrital charcoal samples from gravelly alluvium in our set of 20 radiocarbon samples (Table 1). All three samples yielded anomalously old ages. Our tentative interpretation is that erosion somewhere upstream exposed old charcoal which was then transported down the trough axis and redeposited in the closed depression that we trenched. The underlying two radiocarbon ages are also problematic. Sample Chab 4-5 (unit 5a) lies nearly a meter below sample Chab 4-3 (unit 4c), yet yields a younger age (1,009 to 1,279 cal BP vs 1,343 to1,563 cal BP). In fact, unit 4c's radiocarbon age nearly overlaps at 2-sigma with unit 8's age, despite the fact that it is 1.5 m deeper in the section.

Trench 4, Interpretation

Based on stratigraphic superposition, cross-cutting relationships, and angular unconformities, we interpret a sequence of at least three deformation events at Trench 4 (Table 5 and Fig. 13).

Event Z has the best evidence of rapid vertical displacement and creation of a scarp free face (upward fault truncation at an angular unconformity, scarp-derived colluvial wedge). Its displacement is estimated as 20 cm on F6 (from the offset of unit 6) and 50 cm on F3 (twice the maximum thickness of colluvial wedge unit 7c; McCalpin, 2009). Event Y also has good evidence via the truncation of units 5a-5b and their presence as deformed slivers in the main fault zone (units 5c-5d). However, given Event Y's estimated net slip of 2 m, it should have generated a colluvial wedge deposit roughly 1 m thick. As shown in Stage 5 of Fig. 13, the most proximal part of units 5c and 5d may in fact be this colluvial wedge, shed from the Event Y free face, but later so sheared by displacement in Event Z (50 cm) that it became unrecognizable as a colluvial wedge.

Discussion

Due to the fine scale at which four trenches were logged, our observations on deposit sedimentology and soil formation are detailed enough to define several discrete depositional environments. In vertical section these depositional environments can change, sometimes rather abruptly. The most abrupt changes are usually associated with displacement events on the sackungen faults, recognized by the common indicators used in paleoseismic trenching (upward terminations of faults, colluvial wedges, angular unconformities, block tilting). Below a general model of sedimentation in sackungen troughs is described.

Sedimentation in Sackungen Troughs

Sackungen troughs are sediment traps affected by both climate changes and surface faulting. Due to the low axial slope of most troughs, minor changes in hillslope processes above the trough can change the style of sedimentation in the trough. For example, parts of the trough when initially formed may be closed depressions, filled by temporary ponds. Over time colluvial and slopewash sediments will selectively fill the closed depressions and eventually a through-flowing stream may develop in the trough. Such an evolution is represented in trough stratigraphy by fine-grained sag pond sediments directly overlying the bedrock, and grading upward into fluvial sediments. Conversely, if

Tab. 5.
Inferred sequence of depositional, pedogenic, and deformational events affecting Trench 4.

Event (oldest at bottom)	Evidence
Deposit units 7b-9, develop modern soil (horizons 9A, 10)	Alluvium (unit 7b) fills the deepened trough axis, while scarp-derived colluvium (unit 7c) covers the eroded F3-F4 free face. Thin colluvium (unit 8; **742-937 cal BP**) and more alluvium (unit 9) are deposited in trough. The modern soil A-horizon (unit 9A) and peat layer form.
Deformation EVENT Z	Renewed normal faulting on F3-F6 displaces units 5, 6, and 7a, and deepens the sackungen trough.
Deposit units 5-7a	Unit 5 is deposited as colluvium from the north. Then a small stream flows down the trough axis, depositing units 6 and 7a.
Deformation EVENT Y	Normal faulting on the main fault zone (F3-F6) displaces unit 4 at least 3 m down-to-north. Units on both footwall and hanging wall are rotated down-to-south from sub horizontal to 10-15° south dip. This suggests domino-style faulting.
Deposit units 2-4	Displacement creates a closed depression at the site of Trench 4, after which unit 2 is deposited in a shallow sag pond. Later, talus from upslope (north) fills the sag pond (units 3, 4). All units are subhorizontal.
Deformation EVENT X	Initial sackungen displacement occurs south of Trench 4.

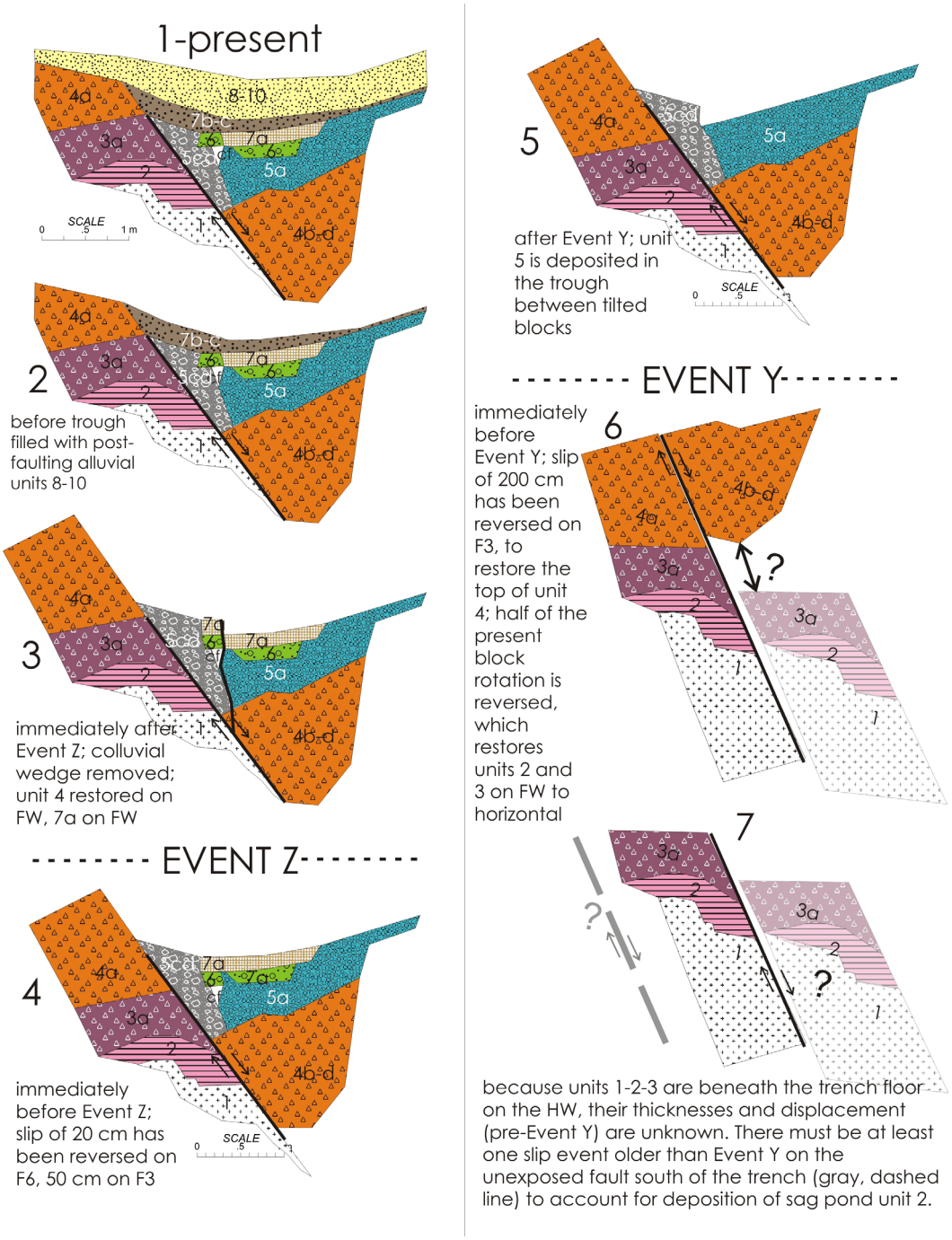

Fig. 13. Retro-deformation sequence of Trench 4. Stage 1 shows the present geometry of strata and structures on the trench wall. Preceding stages are drawn by removing any post-faulting strata (usually on the HW), restoring eroded parts of strata (on the FW), and then reversing the slip on the fault to realign pre-faulting strata tops. This retro-deformation sequence cannot explicitly measure fault slip prior to deposition of unit 4, because the older units (1, 2, and 3 in Stages 6 and 7) are not exposed on both sides of the fault.

the axial slope of the trough is very low, increased colluvial deposition at any point can form a small dam in the trough, which also creates a closed depression. In such a depression the trough stratigraphy would show colluvium directly overlying the bedrock, and being overlain in turn by sag pond sediments.

A second cause of abrupt changes in trough sedimentation is renewed displacement on the sackungen fault, which creates (or deepens) closed depressions and exposes fresh bedrock on the scarp face. Trough stratigraphy will record the abrupt appearance of closed-depression facies (fine-grained sag pond deposits) in areas where previous deposition was colluvial or fluvial. As with tectonic normal faults, fault reactivation results in scarp-derived colluvial wedges near the fault. However, these wedges are smaller than those on tectonic fault scarps, for two reasons: (1) the exposed fault plane is usually bedrock which erodes slowly, compared to a free face in unconsolidated depo-

sits, and (2) trough sediments are derived mainly from upslope or from upgradient in the trough axis, not from the scarp face. Accordingly, sackungen reactivation episodes are more commonly identified by: (1) upward termination of faults at different stratigraphic levels; (2) angular unconformities; (3) abrupt changes in the sedimentology of trough deposits; and (4) burial of soil profiles in the trough (developed during deposition hiatus) by renewed clastic sedimentation.

The climatic and 'tectonic' controls act independently yet synchronously on the scarp-trough system, making it challenging to determine which control is responsible for changes in trough sedimentation. Climate-driven deposition can range from slow and continuous, to episodic separated by hiatuses (soil formation). Likewise, surface displacement can range from slow creep to episodic surface-rupturing events. These two controls form four possible geometries for trough sediments (Fig. 14):

a) continuous deposition and continuous creep, which results in progressively more deformation down section in the trough sediments but a lack of paleosols,
b) continuous deposition combined with episodic fault displacement, which creates "packages" of trough strata bounded by angular unconformities, but without paleosols,
c) episodic deposition and continuous creep, which result in packages of strata bounded by angular unconformities, but each package is topped by a paleosol that represents a long hiatus during which creep continued to deform the underlying package,
d) episodic deposition combined with episodic displacement, which creates packages of strata and paleosols, but soils can appear anywhere within a package, because the two controls operate independently.

All of our trenches show evidence of episodic displacements, and most have buried soils in the trough sediments, so they correspond to Fig. 14d, as follows:

Trench 1: contains independent evidence of rapid displacements: (1) splay faulting cuts unit 5b and 6AB; (2) large granite clasts occur in colluvium (units 4a, 4b), in a much finer matrix, suggesting derivation from a scarp free face; and (3) there is a sudden change from soil formation (6AB) to sag pond conditions (unit 7). By itself the sudden change could be climatic (Fig. 14c), but since it coincides with an upward fault termination, it more likely represents episodic displacement (Fig. 14d).

Trench 2: shows a rapid change from coarse deposition (unit 10d, solifluction) to sag pond deposition (units 11a, 11b, 12). This disconformity could be caused by tectonic causes (i.e., reactivated faulting creates a closed depression) or by climatic causes. However, the disconformity also has a scarp-derived colluvial wedge sitting directly on it (unit 11c) at the main fault, and it forms the upward termination of two faults (F1, F2). Those two features cannot be created by climate changes.

Trench 3: contains structural indicators of episodic displacement. Between faults F2 and F3 units 2h, 4b, and 5b were rotated from subhorizontal (4b is a sag pond deposit) to a northward dip of 30°. All three units have

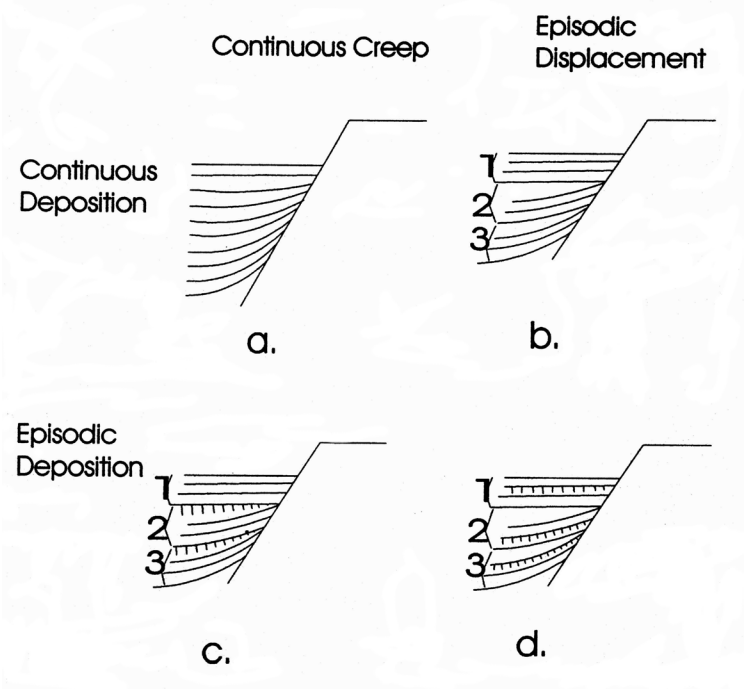

Fig. 14. Hypothetical cross-sections through a sediment-filled trough (at left) adjacent to a sackung scarp (at upper right). In the trough, thin lines indicate bedding, short vertical lines indicate soils. (a) Continuous creep and continuous deposition create a pattern of increasing folding (drag) with depth; no buried paleosols are present. (b) Episodic displacement and continuous deposition result several "packages" of strata bounded by angular unconformities; no buried paleosols are present. The angular unconformities are "event horizons" in the terminology used by paleoseismologists. (c) Continuous creep and episodic deposition yield several unconformity-bounded packages of strata. Each package is topped by a paleosol, the upper parts of which have been eroded nearest the sackung fault plane. The upper contact of each paleosol is an event horizon. (d) Episodic displacement and episodic deposition yield discrete unconformity-bounded packages of strata, but paleosols may be found at any position within the stratigraphic sequence. In this scenario, the angular unconformities are event horizons, which do not coincide with the paleosols. From McCalpin, 2003.

been rotated the same amount despite their difference in age, which is incompatible with creep displacement. The overlying units 5b and 6b are horizontal, forming a strong angular unconformity. There cannot be significant age difference between the youngest rotated stratum (5b) and the oldest unrotated stratum (6a), because closer to the main fault (F4) their correlatives (units 5a, 6b) lie conformably atop each other. Thus, the rotation of units 2h-4b-5b must have taken place in a very short time. There has been no movement on F3 since that time, which rules out fault creep.

Trench 4: has indicators of episodic displacement similar to Trench 2. There is a disconformity between units 5d-6-7a and units 7b-7c. Both units 7a and 7b are alluvium, so it could be argued that the disconformity was climatically induced. However, the disconformity also truncates faults F3, F4, F5, and F6 and has a colluvial wedge (unit 7c) sitting directly on it. Those features suggest the disconformity is tectonic.

Radiocarbon Dating of Sackungen

Table 1 (footnotes 3, 4, and 5) and the geochronology section for each trench describe some of the ambiguities in radiocarbon dating of sackungen trough sediments. We observed problems with three types of samples, described below.

Radiocarbon samples from shear zones

We dated carbon samples from shear zones in Trench 1 (Chab 1-4), Trench 2 (Chab 2-9), Trench 3 (Chab 3-3). This followed the practice from the early days of paleoseismic trenching, of dating any carbon found in a trench, especially near the fault. It was assumed then that all carbon in the fault zone had been dragged up (or fallen in) during the most recent displacement event (MRE), so its age would set a close maximum age constraint on the MRE. Sample Chab 1-4 dated at 2,380 to 2,755 cal BP, which was much older than the most recent movement in Trench 1. Sample Chab 2-9 dated at 3,446 to 3,690 cal BP, also older than the most recent event in Trench 2 (≥1.6-1.8 ka). Sample Chab 3-3 dated at 2,491 to 2,945 cal BP, compared to the youngest displacement even there of <1.7-1.9 ka. It then became obvious that the carbon in the shear zone could have one of two origins. First, it could represent surface soil carbon that fell into a crack or fissure at the time of a displacement event. In this case, the carbon would closely date a displacement event, but not necessarily the most recent one. This is especially likely for samples deep in the shear zone. Second, the carbon in trough deposits occurs as burn layers (charcoal) or as buried organic soil horizons. If this carbon is dragged up into the fault zone, its radiocarbon age reflects the age of sediment deposition or soil formation, not the age of the later displacement event that dragged it into the shear zone. We finally decided that most radiocarbon ages from shear-zones could not be associated with a specific displacement event, or interpreted as a minimum versus maximum age constraint.

Radiocarbon samples from thin silt films on talus clasts

Several of our trenches contained deposits composed angular pebble-sized rock fragments with no matrix (openwork texture) that we interpreted as talus (Trench 3, units 5b, 11a). If these deposits were located beneath the axis of the trough, the clasts were stained black, unlike all other units. The black stain was a thin coating of black silt/clay that could be rubbed off with the fingers. It is not clear whether the black stains are primary depositional features, or younger illuviated components deposited by organic-rich groundwater. Radiocarbon ages from these stains are anomalously young compared to the ages charcoal or soil organics in nearby stratigraphic units. We suspect that water standing in the trough infiltrated down through the A-horizon of the surface soil, entraining the black silt, and then carried it downward and redeposited it in the water-filled pore spaces of the openwork gravels.

Radiocarbon samples from scarp-face soils and scarp-derived colluvium

In the dynamic environment of sackungen scarps and troughs, old soils can be faulted upward, exposed at the top of a scarp free face, and then eroded and re-deposited into the colluvial wedge at the base of the free face. This process recycles old carbon from the faulted soil into the newly-deposited, post-faulting colluvial wedge, resulting in an anomalously old radiocarbon age for the wedge. That age is commonly older than the radiocarbon ages of the deposits underlying the colluvial wedge, such as occurs on Scarp 4B of Trench 3. There, soil 8A/8AB3 (9.3-9.6 ka) was upfaulted and tilted on Block I, eroded off the top of Scarp 4B, and redeposited into the much younger unit 14A, which on stratigraphic grounds is only slightly older than 1.7-1.9 ka. But the radiocarbon sample from 14A dated much older at 9.0-9.4 ka. In theory, a similar process could occur if the axial drainage in the trough undermined a soil-capped streambank, and pieces of an old organic soil fell into the alluvium.

Small-Scale Evolution of Sackungen Surface Deformation

Our two trenches on Scarp 4 revealed a complex evolution of structures over a small area, which contains two antislope scarps (4A, 4B) with an intervening structural

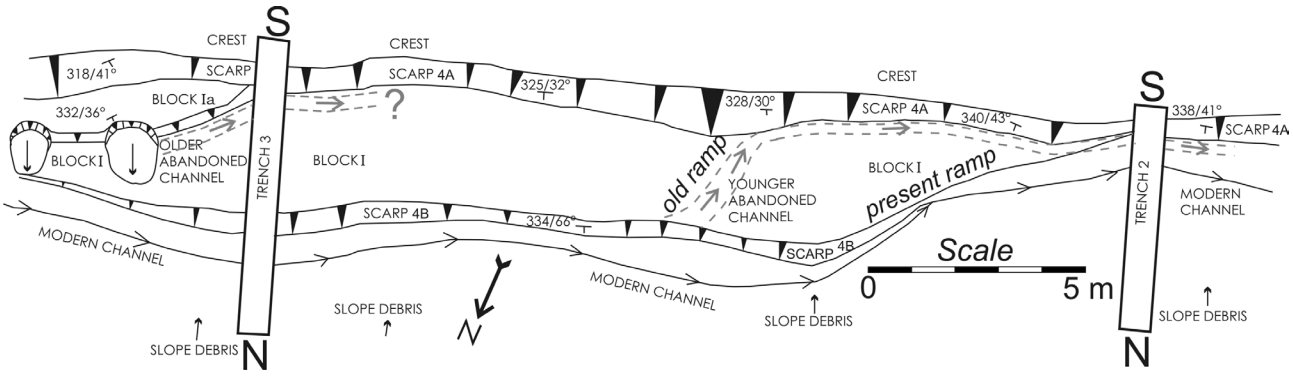

Fig. 15. Geomorphic sketch map of Scarp 4 in the vicinity of Trenches 2 and 3; north is toward bottom left. Triangles on scarp faces point downslope; strike/dip symbol and labels reflect the orientation of the scarp face. Scarp 4A (the main scarp) and Scarp 4B (subsidiary scarp) bound a structural block that we call Block I. The top of Block I forms a ramp structure (present ramp) that dives beneath the trough floor east of Trench 2.

block (Block I; Fig. 15). The modern channel in the sackungen trough flows west along the toe of Scarp 4B. At the western end of Block I, Scarp 4B dies out and the surface of Block I plunges beneath the trough floor in a fault ramp. The modern channel then follows the end of this ramp on an oblique path to the toe of Scarp 4A.

The western part of Block I is crossed by an abandoned, partially infilled channel with the same width and oblique orientation as the modern channel. This channel has been uplifted and truncated by Scarp 4B, which caused its abandonment. We infer that this "younger abandoned channel" marks a former location where the Block I ramp (old ramp) once plunged beneath the trough floor, and the stream at that time followed the toe of that ramp. Subsequently Block I has risen and both Scarp 4B and Block I have grown westward. As Scarp 4B continues to grow westward, its will eventually defeat the oblique reach of the modern channel and force the channel northward, thus truncating the modern channel and creating another abandoned channel segment on Block I. Farther east at the toe of Block Ia there is an even older abandoned channel, which has no surface expression, but is exposed in Trench 3.

Deposits of both the modern and older abandoned channels are exposed in Trench 3, whereas Trench 2 exposes the modern and younger abandoned channels (Fig. 16). The basal deposits of the younger abandoned channel date at 1,625 to 1,870 cal BP and the soil A-horizon overlying the channel dates at 331 to 631 cal BP. Soil development is weak, consisting of only a organic A-horizon, which is consistent with the channel's young geomorphic expression and radiocarbon ages. In contrast, deposits of the older abandoned channel in Trench 3 carry a well-developed soil profile consisting of A, AB, and textural B-horizons. The base of horizon 8AB yielded an age of 9,280 to 9,662 cal BP (early Holocene), which is consistent with the degree of soil formation, and with the fact this paleo-channel has no surface expression. Overall, trench exposures confirm the spatial/temporal scenario suggested by the surface geomorphology. We now see that, as fault blocks and ramps develop and grow laterally in a sackungen trough, their emergence forces the trough depocenter to migrate laterally, shifting the locus of sag pond deposition and fluvial facies. Likewise, on rising fault blocks sedimentation changes from sag pond to fluvial, and then to aeolian and soil formation once the block is abandoned by trough sedimentation.

Large-Scale Evolution of Sackungen Surface Deformation

Previous research on swarms of parallel sackungen have documented that scarps at higher elevations formed later (known as "onset age"). Hippolyte et al. (2009) concluded: "*This decrease of the age of the scarps with elevation much probably reflects the propagation of the deformation toward the crest (from elevation 2,190 m to 2,419 m)... This chronology agrees with the proposed mechanism of flexural toppling. The migration of the slope deformation from the valley flank to the crest also supports the model of glacial debuttressing for the origin of the Arcs sackungen*." Pánek and Klimeš (2016) concluded "*In general, we observe a statistically significant correlation showing a progressive decrease of sackungen scarp* [onset] *ages with their increasing altitudinal position... Such a relationship might indicate linkage of (delayed) sackungen genesis to overall thinning and retreat of glaciers since the LGM… Therefore, slow upslope migration of stress release after glacier withdrawal… could partly explain substantial time lag of a number of sackungen scarps*."

The younger displacement events in our Chabenec trenches do not show this trend. In Fig. 17 we compare the ages of displacement events amongst the trenches over the past 6 ka (older events have too few radiocarbon ages and

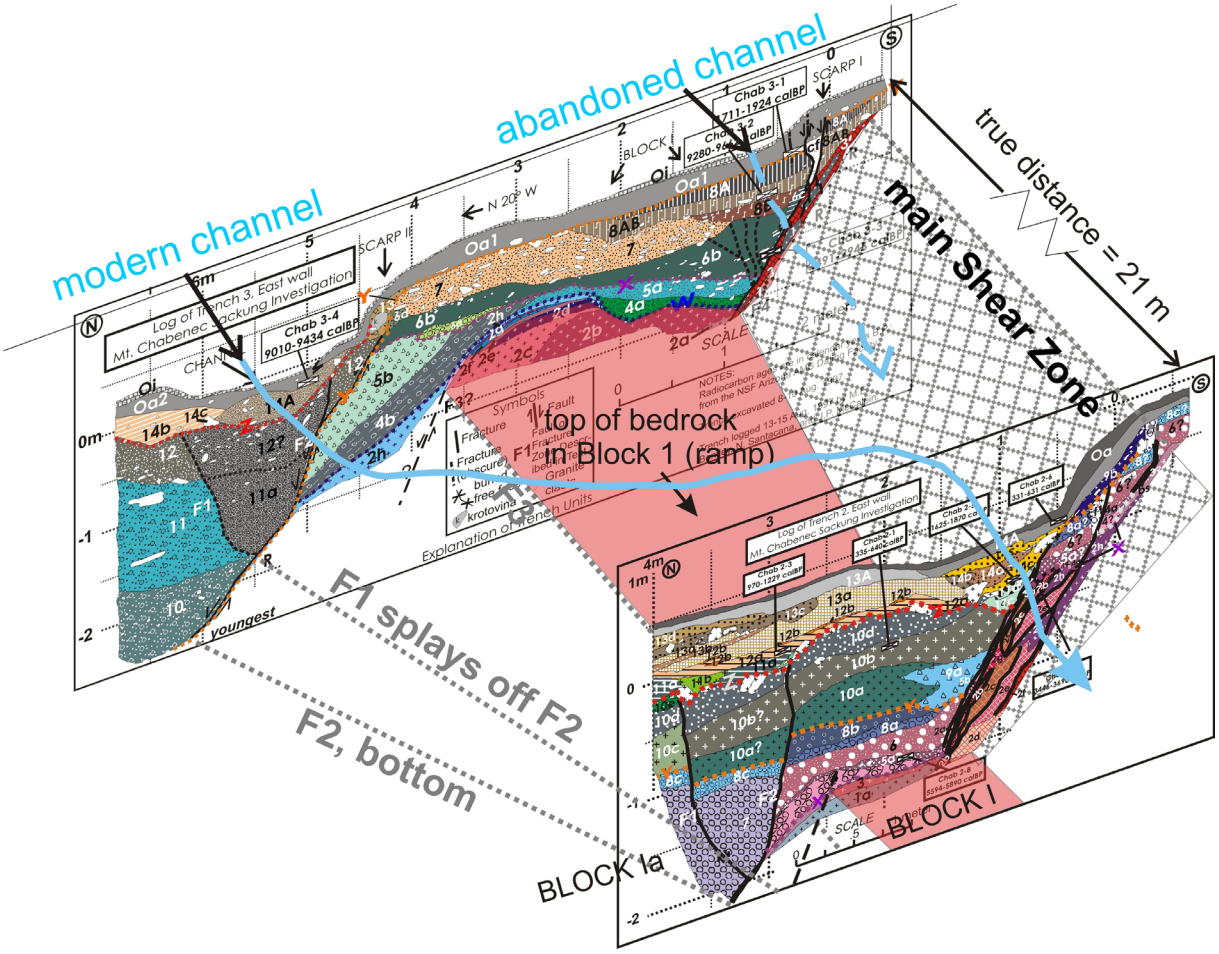

Fig. 16. Pseudo-isometric diagram of the Trenches 2 and 3, with distance between the trenches shortened from true scale. North is to the left. The top of bedrock in Block I is highlighted in red, plunging down to the west. Thick light blue lines indicate the modern and abandoned channel thalwegs.

are too affected by contamination processes; see section 5.2). The most striking pattern is that, in all four trenches, there is a displacement event between ca. 1 and 2 ka.

In paleoseismic trenches across normal faults, the maximum limiting radiocarbon age on a faulting event typically forms a closer age constraint than the minimum limiting age. This is because the dated carbon typically comes from a soil horizon that was rapidly buried by post-faulting deposition (McCalpin, 2009). Maximum limiting ages on events Y_1, Z_2, Z_3, and Z_4 are surprisingly similar (1,860 cal BP; 1,720 cal BP; 1,820 cal BP; and 1,410 cal BP, respectively).The ages are not strictly synchronous, but neither do they show a pattern of younger events at higher elevations. Therefore, a common trigger mechanism cannot not be ruled out.

Trigger Mechanism

Three trigger mechanisms are normally considered for episodic sackungen displacements, two exogenetic and one endogenetic: (1) seismic shaking, (2) extreme precipitation events, or (3) a slow uphill advance of tensional stress caused by glacial oversteepening of lower slopes (Pánek et al., 2015). Not surprisingly, workers in seismically-active regions prefer trigger 1 (e.g., Italy; Carpathian Mountains; Caucasus Mountains; New Zealand; California, USA), attributing sackung formation to either direct surface rupture or to seismic shaking (e.g., photographs in Khromovskikh, 1989; see also Zischinsky, 1966; Beck, 1968; Radbruch-Hall et al., 1976; Mahr, 1977). For example, Salvi and Nardi (1995, p. 107-108) state"*... strong ground shaking associated with earthquakes is one of the main triggering factors for the growth of 'sackungen-like' features*". This contention is partly based on the appearance of new antislope scarps in hilly terrain after moderate-to-large-magnitude earthquakes (e.g., Dramis and Sorriso-Valvo, 1983; Morton and Sadler, 1989; Morton et al., 1989; Cotton et al., 1990; Ponti and Wells, 1991; Nolan and Weber, 1992; Blumetti, 1995; Jibson et al., 2004; Moro et al., 2007), and partly on a spatial association of sackungen

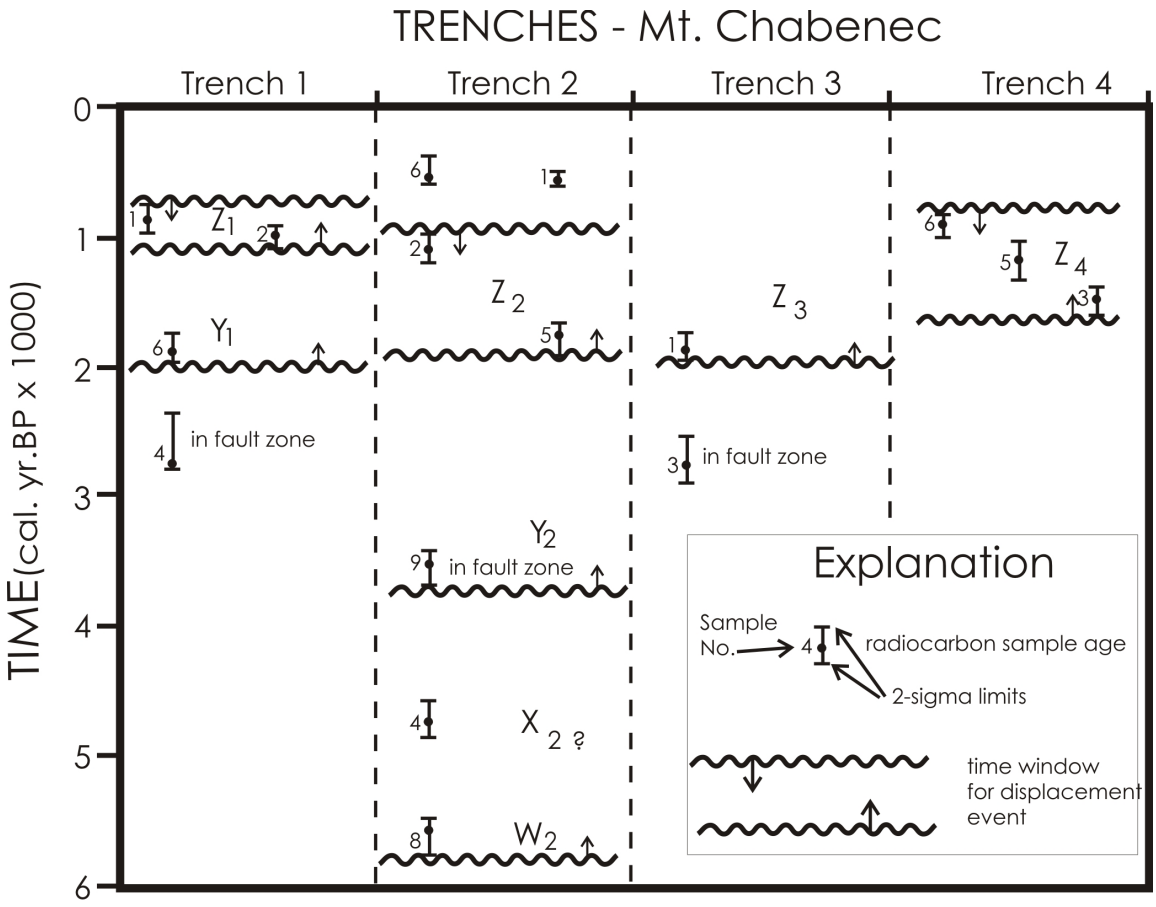

Fig. 17. Space-time diagram of displacement events observed in the four trenches. Z1 is the latest event in Trench 1; Y1, is the penultimate event in Trench 1, etc. Calendar-corrected ages are from Table 1.

with active fault traces. Criteria for testing possible trigger mechanisms are summarized by McCalpin (1999, 2003). In contrast, workers in glaciated mountains tend to favor trigger 3. An example is Pánek et al. (2017), who state that sackungen in the High Tatras are unlikely to be triggered by seismicity, given the low seismicity rates in the historic record. Instead, they conclude that: "*slow upslope migration of stress release after glacier withdrawal… could partly explain substantial time lag of a number of sackungen scarps*."

To assess the possibility of seismic triggering, we must consider the seismotectonic setting of Mount Chabenec. Our latest sackungen displacements date just younger than 1,410-1,860 cal yr BP (i.e., 140-590 A.D). Unfortunately, the earthquake history of northern Slovakia-southern Poland extends only back to 1259 A.D. (the 31-JAN-1259 earthquake; Io=7, Mw=5, at approx. 49.9N, 19.25W; Grunthal et al., 2009). The felt area in 1259 included "*Poland, Bohemia, Hungary, Russia, Leczyca, etc*." (Guterch and Kozak, 2015). The 1259 earthquake is hundreds of years too recent to be the trigger mechanism for the MRE displacements on Mount Chabenec, but it does demonstrate that seismic ground motions can occur at our study site, from moderate-magnitude regional earthquakes.

Mount Chabenec lies within the Čertovica seismotectonic zone (Fig. 18), one of four 'seismoactive zones' defined in Slovakia by Kováč et al. (2002), Hók et al. (2016). They describe the Čertovica line as follows: *"The Čertovica line is a surface projection of the thrust plane of the Veporic basement sheet over the Tatricum. Based on geological data, earthquake focal mechanisms (Pospíšil et al., 1992), geophysical data (Bezák et al., 1993, 1995; Šefara et al., 1998) and structural analyses (Hók et al., 1997, 1999, 2000) we consider this sector of the Čertovica Line as a recently active due to extensional collapse of the orogene. Earthquake events are released mostly on the Hron fault system of ENE-WSW direction... It is noteworthy that this system, like the Dobrá Voda system, is distinctive in the recent morphology and can be well traced by remote sensing methods (Janků et al., 1984)".* The active Hron fault system mentioned above extends within 10 km south of Chabenec's summit.

Historic earthquakes in the Čertovica zone have clustered at the western end near Banská Bystrica and at

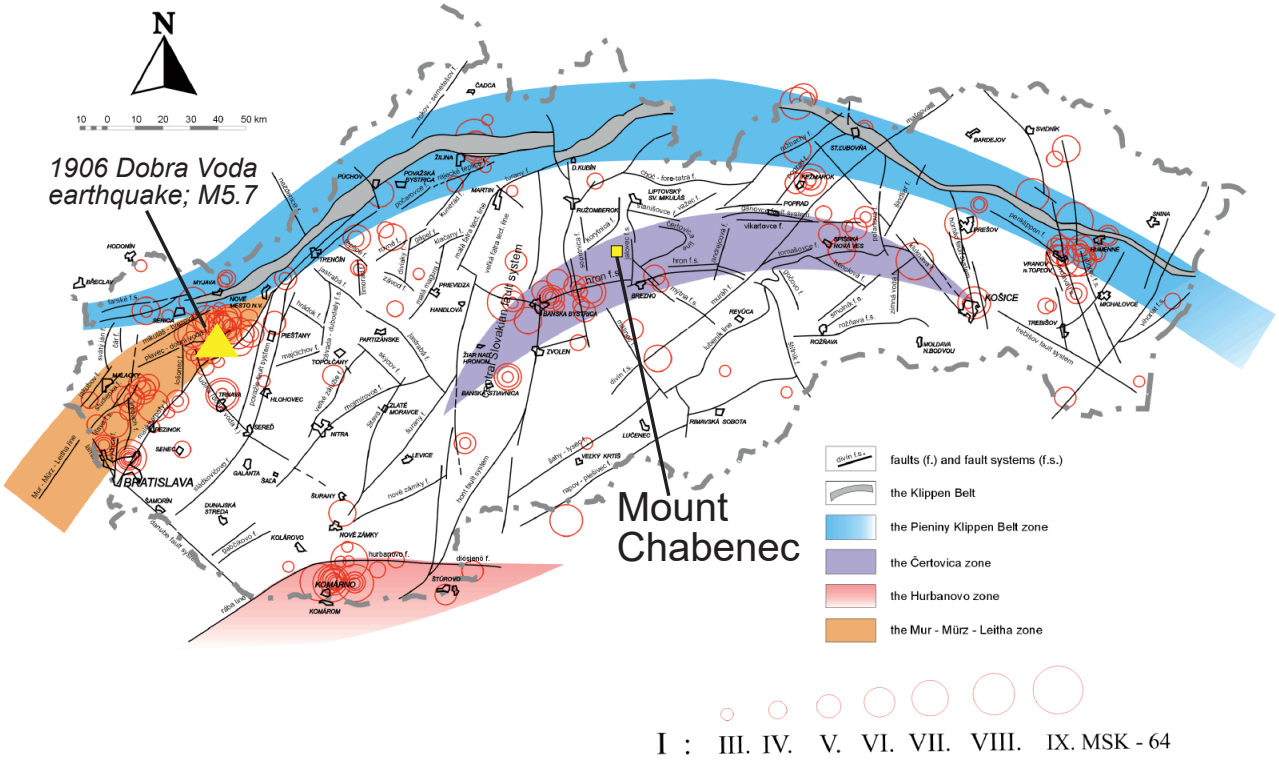

Fig. 18. Seismically active zones of the Western Carpathians with indicated epicenters of earthquakes for the period 1034–1990 and position of the seismotectonic zones. Mount Chabenec (yellow square) lies in the Čertovica seismotectonic zone, which contains the active Hron fault between Mount Chabenec and Banská Bystrica. The largest earthquake in the 20th century (1906 Dobrá Voda) is shown as a yellow triangle. Modified from Kováč et al., 2002.

the eastern end, with a "seismic gap" in the center. The former earthquakes include one of the largest instrumental events in the Slovakia (the M4.3 earthquake of 07-JUNE-1989; 48.779°N, 19.21°E) which occurred only 27 km southwest of Mount Chabenec. Recent neotectonic studies have discovered possible late Quaternary fault movements on the northern flank of the Nízke Tatry Mountains, not far NE of Chabenec. Vojtko et al. (2011) identified 130 ka alluvium apparently displaced by the 55 km-long Vikartovce fault, an E-W structure on the north side of the Nízke Tatry range. The west end of this south-dipping normal fault lies only 40 km NE of the Chabenec summit. Closer to Chabenec, Littva and Hók (2014) infer late Quaternary fault displacements in the NNE-trending Jánska dolina Valley, only 10 km NE of Chabenec. This trend, if projected southward, would approach even closer to the Chabenec sackungs. Neither of these studies included paleoseismic trenching or dating of individual paleoearthquakes, so there is currently no way to test if those faults moved between 1,410 to 1,860 cal yrs BP.

None of the neotectonic data above conclusively prove that seismic shaking triggered the sackungen reactivations between 1 and 2 ka. To test that hypothesis would require knowing if there had been active faulting events or strong shaking events in the vicinity of Chabenec in the 1-2 ka period. Such detailed data can only come from paleoseismic chronologies of regional active faults or of secondary shaking features such as liquefaction or lateral spreads, but such chronologies do not exist yet for northern Slovakia.

Conclusions

We applied paleoseismic trenching techniques to four trenches dug across three antislope scarps on the south ridge of Mount Chabenec. Beneath the scarps is a complex shear zone in granodiorite, 25-50 cm thick, dipping 55-60° N (into the slope). The shear zones contain multiple fault strands, gouge zones, and alteration zones suggestive of deep crustal shear rather than shallow extensional faulting. The implication is that ongoing deep-seated, gravitational toppling deformation is utilizing old pre-Quaternary fault zones. Structure and stratigraphy exposed in the trenches are consistent with episodic slip on the sackungen faults coupled with episodic deposition and soil formation in the adjacent troughs. Rapid changes in sedimentation style and cessation of soil formation correlate stratigraphically with episodes of displacement on the sackungen structures. Despite this correspondence of episodic displacement

and sedimentation, we encountered difficulties in dating displacement events with radiocarbon. Five of our 20 samples yielded inverted ages, due either to recycling old carbon within the trough, or to contaminating porous old deposits with carbon from overlying, younger deposits. In hindsight, we should have supplemented radiocarbon dating with luminescence dating, which would have been possible because every trough contained one or more fine-grained, sag pond deposits.

Radiocarbon ages indicate that in all four trenches, there was a displacement event in the late Holocene (shortly after 1,410 to 1,860 cal yrs BP). The longest well-dated record in a single trench (Trench 2) contained four inferred displacement events in the past 6 ka, yielding a long-term average recurrence of ca. 1.5 ka. These four events have created an antislope scarp with ~5 m of vertical surface offset. The near-synchroneity of the late Holocene displacements stands in contrast to other dated sackungen sites, where displacements become younger with increasing elevation. Having near-synchronous displacement events at multiple elevations suggests an external trigger, either climatic or seismic. Unfortunately, there is no record of regional paleoearthquakes or meteorological events between 1-2 ka to further test that hypothesis.

Acknowledgements

Stan Novosad (Denver, CO) first told JPM about the classic sackungen at Mt. Chabenec and helped to plan our trenching campaign. PL and RJ coordinated all the field logistics. Thanks to our valiant trenching crew (Fig. 19) who ascended 600 m to the trench sites; dug the trenches; and descended back to base camp for 10 consecutive days.

References

Agliardi, F., Crosta, G. B., Zanchi, A. & Ravazzi, C., 2009: Onset and timing of deep-seatedgravitational slope deformations in the eastern Alps, Italy. *Geomorphol., 103, 113 – 129.*

Bagge, M. & Hampel, A., 2016: Three-dimensional finite-element modeling of coseismic Coulomb stress changes on intra-continental dip-slip faults. *Tectonophysics, 684, 52 – 62.*

Beck, A. C., 1968: Gravity faulting as a mechanism of topographic adjustment. *New Zealand J. Geol. Geophys., 11, 191 – 199.*

Beget, J. E., 1985: Tephrochronology of antislope scarps on an alpine ridge near Glacier Peak,Washington, USA. *Arct. Alpine Res., 17, 143 – 152.*

Bezák, V., Hók, J., Kováč, P. & Madarás, J., 1993: Possibilities of tectonic interpretation of the seismic section 2T (in

Fig. 19. Field team of the Chabenec trenching project. Red arrows indicate sackungen scarps on the southern slope of Mt. Chabenec. View to the east: 1-Nuria Santacana, Tech. Univ. of Catalonia; 2-Molly Bentley Zorba, Univ. of Colorado; 3-Juraj Michalko, SGIDS; 4-Stanislav Petruška†; 5-Tibor Vlník; 6-Pavel Liščák, SGIDS; Not pictured: Robert Jelínek and Jozef Hók, SGIDS; Gustáv Gabauer†, J. P. McCalpin, GEO-HAZ Consulting (photographer). † indicates deceased.

Slovak, English abstract), In: Rakús, M. and Vozár, J. (Eds.): Geodynamic model and deep structure of the western Carpathians. Konf., Symp., Sem. *Bratislava, Geol. Úst. D. Štúra, 287 – 290.*

Biely, A., Beňuška, P., Bezák, V., Bujnovský, A., Halouzka, R., Ivanička, A., Kohút, M., Klinec, A., Lukáčik, E., Maglay, J., Miko, O., Pulec, M., Putiš, M. & Vozár, J., 1992: Geological map of the Nízke Tatry Mountains 1 : 50,000. Bratislava, SGÚ – Geol. Úst. D. Štúra.

Blumetti, A. M., 1995: Neotectonic investigations and evidence of paleoseismicity in theepicentral area of the January – February 1703, central Italy, earthquakes. In: Serva, L. and Slemmons, D. B. (Eds.): Perspectives in Paleoseismology. *Assoc. Engin. Geol. Spec. Publ., 6, 83 – 100.*

Carbonel, D., Gutierrez, F., Linares, R., Roque, C., Zarroca, M., McCalpin, J. P., Guerrero, J. & Rodriguez, V., 2013: Differentiating between gravitational and tectonic faults by means of geomorphological mapping, trenching, and geophysical surveys; The case of the Zenzano fault (Iberian Chain, N Spain). *Geomorphol., 189, 93 – 108.*

Cotton, W. R., Fowler, W. L. & Van Velsor, J. E., 1990: Coseismic bedding plane faults and ground fissures associated with the Loma Prieta earthquake of 17 October 1989, In The Loma Prieta (Santa Cruz Mountains) California, earthquake of 17 October 1989. *Calif. Div. Mines Geol., Spec. Publ., 104, 95 – 103.*

Dramis, F. & Sorriso-Valvo, M., 1983: Two cases of earthquake-triggered gravitational spreading in Algeria and Italy. *Rendic. Soc. Geol. Italia, 6, 7 – 10.*

Gori, S., Falcucci, E., Dramis, F., Galadini, F., Galli, P., Giaccio, B., Messina, P., Pizzi, A., Sposato, A. & Cosentino, D., 2014: Deep-seated gravitational slope deformation, large-scale rock failure, and active normal faulting along Mt. Morrone (Sulmona basin, Central Italy); Geomorphological and paleoseismological analyses. *Geomorphol., 208, 88 – 101.*

Guterch, B. & Kozak, J. (Eds.), 2015: Studies of historical earthquakes in southern Poland. *Springer Publ., 179 p.*

Gutierrez, F., Acosta, E., Rios, S., Guerrero, J. & Lucha, P., 2005: Geomorphology and geochronology of sackungen features (uphill-facing scarps) in the Central Spanish Pyrenees. *Geomorphol., 69, 298 – 314.*

Gutierrez, F., Ortuno, M., Lucha, P., Guerrero, J., Acosta, E., Coratza, P., Piacentini, D. & Soldati, M., 2008: Late Quaternary episodic displacement on a sackungen scarp in the central Spanish Pyrenees; Secondary paleoseismic evidence? *Geodin. Acta, 21, 187 – 202.*

Hippolyte, J.-C., Bourlès, D., Braucher, R., Carcaillet, J., Léanni, L., Arnold, M. & Aumaitre, G., 2009: Cosmogenic ^{10}Be dating of a sackungen and its faulted rock glaciers, in the Alps of Savoy (France). *Geomorphol., 108, 312 – 320.*

Hók, J., Kováč, P., Madarás, J., Maglay, J., Kováč, M., Baráth, I., Sabol, I., Slávik, M. & Lukaj, M., 1997: Neotectonic and geomorphological evolution of the territory of Slovakia, part Geology (in Slovak). *Manuscript. Bratislava, archive St. Geol. Inst. D. Štúr, 1 – 77.*

Hók, J., Kováč, M., Kováč, P., Nagy, A. & Šujan, M., 1999: Geology and tectonics of the NE part of the Komjatice depression. *Slovak Geol. Mag., 5, 187 – 199.*

Hók, J., Bielik, M., Kováč, P. & Šujan, M., 2000: Neotectonic character of Slovakia (in Slovak, English summary). *Miner. Slov., 32, 459 – 470.*

Hók, J., Kysel, R., Kováč, M., Moczo, P., Kristek, J., Kristeková, M. & Šujan, M., 2016a: A seismic source zone model for the seismic hazard assessment of Slovakia. *Geol. Carpath., 67, 3, 273 – 288.*

Jahn, A., 1964: Slope morphological features resulting from gravitation. *Zeit. Geomorphol. Suppl. Bd., 5, 59 – 72.*

Janků, J., Pospíšil, L. & Vass, D., 1984: Contribution of remote sensing to the knowledge of West Carpathians structure (in Slovak, English summary). *Miner. Slov., 16, 121 – 137.*

Jibson, R. W., Harp, E. L., Schulz, W. & Keefer, D. K., 2004: Landslides triggered by the 2002 Denali Fault, Alaska, earthquake and the inferred nature of the strong shaking. *Earthquake Spectra, 20, 669 – 691.*

Khromovskikh, V. S., 1989: Determination of magnitudes of ancient earthquakes from dimensions of observed seismodislocations. *Tectonophysics, 166, 1 – 12.*

Kováč, M., Bielik, M., Hók, J., Kováč, P., Kronome, B., Labák, P., Moczo, P., Plašienka, D., Šefara, J. & Šujan, M., 2002: Seismic activity and neotectonic evolution of the Western Carpathians (Slovakia). *EGU Stephan Mueller Spec. Publ. Ser., 3, 167 – 184.*

Littva, J. & Hók, J., 2014: Neotectonics of the Inner Western Carpathians; Liptovský Ján area, case study (northern slopes of the Nízke Tatry Mts., Slovakia). *Acta Geol. Slov., 6, 2, 123 – 134.*

Mahr, T., 1977: Deep-reaching gravitational deformations of high mountain slopes. *Bull. Engr. Geol. Environ., 16, 121 – 127.*

Mahr, T. & Nemčok, A., 1977: Deep-seated creep deformations in the crystalline cores of the Tatry Mountains. *Bull. Engr. Geol. Environ., 16, 104 – 106.*

Mariotto, F. P. & Tibaldi, A., 2016: Inversion kinematics at deep-seated gravity slope deformations revealed by trenching techniques. *Nat. Haz. Earth Syst. Sci., 16, 663 – 674.*

Mazúr, E. & Lukniš, M., 1986: Regionálne geomorfologické členenie Slovenska 1 : 500 000 [Regional Geomorphological Division of Slovakia 1 : 500,000]. *Bratislava, Geogr. Úst. Slov. Akad. Vied.*

McCalpin, J. P., 1999: Criteria for determining the seismic significance of sackungen and other scarplike landforms in mountainous regions. In: Techniques for Identifying Faults and Determining Their Origins, U.S. Nuclear Regulatory Commission, Washington, DC, NUREG/CR-5503, A-122 – A-142.

McCalpin, J. P., 2003: Criteria for determining the seismic significance of sackungen and other scarplike landforms in mountainous regions. In: Hart, E.W. (Ed.): Ridge-Top Spreading in California; Contributions toward understanding a significant seismic hazard. *California Geol. Surv., CD 2003-05, 2 CD-ROMs.*

McCalpin, J. P., 2009: Paleoseismology of Extensional Tectonic Environments, Chapter 3. In: McCalpin, J. P. (ed.): Paleoseismology. 2nd Ed. *New York, Academic Press, 171 – 269.*

McCalpin, J. P., 2013: Trenching and Exposed Faces. In: Shroder, J. F., Switzer, A. D. and Kennedy, D. M. (Eds.): Treatise on Geomorphology, Vol. 14, Methods in Geomorphology. *San Diego, CA, Academic Press, 138 – 149.*

McCalpin, J. P., Bruhn, R. L., Pavlis, T. L., Gutierrez, F., Guerrero, J. & Lucha, P., 2011: Antislope scarps, gravitational spreading, and tectonic faulting in the western Yakutat microplate, south coastal Alaska. *Geosphere, 7, 5, 1 143 – 1 158.*

McCalpin, J. P. & Hart, E. W., 2003: Ridge-top spreading features and relationship to earthquakes, San Gabriel Mountains Region, Southern California – Part B: Paleoseismic investigations of ridge-top depressions. In: Hart, E. W. (Ed.): Ridge-Top Spreading in California; Contributions toward understanding a significant seismic hazard. *California Geol. Surv., CD 2003-05, 2 CD-ROMs.*

McCalpin, J. P. & Irvine, J. R., 1995: Sackungen at Aspen Highlands Ski Area, Pitkin County, Colorado. *Environ. Engin. Geosci., 1, 3, 277 – 290.*

Moro, M., Saroli, M., Gori, S., Falcucci, E., Galadini, F. & Messina, P., 2012: The interaction between active normal faulting and large scale gravitational mass movements revealed by paleoseismological techniques: A case study from central Italy. *Geomorphol., 151, 164 – 174.*

Moro, M., Saroli, M., Salvi, S., Stramondo, S. & Doumaz, F., 2007: The relationship between seismic deformation and deep-seated gravitational movements during the 1997 Umbria-Marche (central Italy) earthquakes. *Geomorphol., 89, 3 – 4, 297 – 307.*

Morton, D. M. & Sadler, P. M., 1989: The failings of the Pelona Schist; landslides and sackungen in the Lone Pine Canyon and Wrightwood areas of the eastern San Gabriel Mountains, southern California. In: Sadler, P. M. and Morton, D. M. (Eds.): Landslides in a semi-aridenvironment, with emphasis on the inland valleys of southern California. *Inland Geol. Soc., Publ., 2, 301 – 322.*

Morton, D. M., Campbell, R. H., Jibson, R. W., Wesson, R. L. & Nicholson, C., 1989: Ground fractures and landslides produced by the North Palm Springs, California, earthquake of July 8, 1986. In: Sadler, P. M. and Morton, D. M. (Eds.): Landslides in a semi-arid environment, withemphasis on the inland valleys of southern California. *Inland Geol. Soc., Publ., 2, 183 – 196.*

Nemčok, A., 1972: Gravitational slope deformation in high mountains. *Proc. 24th Int. Geol. Congress, 13, 132 – 141.*

Nemčok, A., 1982: Zosuvy v slovenských Karpatoch [Landslides in the Slovak Carpathians]. *Bratislava, VEDA, Slovak Acad. Sci. Publ., 318 p.*

Nolan, J. M. & Weber, G. E., 1992: Evaluation of ground cracking caused by the 1989 Loma Prieta earthquake, Santa Cruz County, California; case histories. In: Sharma, S. (Ed.): Proc. 28th Symp. Engin. Geol. Geotech. Engin. *Boise, Idaho, Boise State Univ., 272 – 286.*

Onida, M., Galadini, F. & Forcella, F., 2016: Application of paleoseismological techniques to the study of late Pleistocene-Holocene deep-seated gravitational movements at the Mortirolo Pass (central Alps, Italy). *Netherlands J. Geosci., 80, 209 – 227.*

Pánek, T. & Klimeš, J., 2016: Temporal behavior of deep-seated gravitational slope deformations. *A rev. Earth. Sci. Rev., 156, 14 – 38.*

Pánek, T., Mentlík, P., Ditchburn, B., Zondervan, A., Norton, K. & Hradecký, J., 2015: Are sackungen diagnostic features of (de)glaciated mountains? *Geomorphol., 248, 396 – 410.*

Pánek, T., Mentlík, P., Engel, Z., Braucher, R., Zondervan, A. & The Aster Team, 2017: Late Quaternary sackungen in the highest mountains of the Carpathians. *Quat. Sci. Rev., 159, 47 – 62.*

Pánek, T., Tábořík, P., Klimeš, J., Komárková, V., Hradecký, J. & Šťastný, M., 2011: Deep-seated gravitational slope deformations in the highest part of the Czech Flysch Carpathians; Evolutionary model based on kinematic analysis, electrical imaging, and trenching. *Geomorphol., 129, 92 – 112.*

Ponti, D. J. & Wells, R. E., 1991: Off- fault ground ruptures in the Santa Cruz Mountains, California – ridge-top spreading versus tectonic extension during the 1989 Loma Prieta Earthquake. *Bull. Seismol. Soc. Amer., 81, 1 480 – 1 510.*

Pospíšil, L., Buday, T. & Fusán, O., 1992: Neotectonic movements in the Western Carpathians (in Slovak, English summary). *Západ. Karpaty, Sér. Geol., 16, 65 – 84.*

Radbruch-Hall, D. H., Varnes, D. J. & Savage, W. Z., 1976: Gravitational spreading of steep-sided ridges ("sackungen") in western United States. *Bull. Int. Assoc. Engin. Geol., 14, 23 – 35.*

Reimer, P. J. & 27 others, 2013: IntCal13 and MARINE13 radiocarbon age calibration curves 0-50000 years cal BP. *Radiocarbon, 55, DOI: 10.2458/azu_js_rc.55.16947.*

Salvi, S. & Nardi, A., 1995: The Ovindoli fault; a segment of a longer, active fault zone in central Abruzzi, Italy. In: Serva, L. & Slemmons, D. B. (Eds.): Perspectives in Paleoseismology. *Assoc. Engin. Geol. Spec. Publ., 6, 101 – 113.*

Šefara, J., Kováč, M., Plašienka, D. & Šujan, M., 1998: Seismogenic zones in the Eastern Alpine-Western Carpathian-Pannonian Junction area. *Geol. Carpath., 49, 247 – 260.*

SGIDS, 2018: 1 : 50,000-scale geological maps of the Slovak Republic: State Geol. Inst of Dionýz Štúr, on-line map server at, accessed 13-Jan-2018.

Soil Survey Staff, 2014: Keys to Soil Taxonomy. *Washington, DC, US Dept. Agriculture-Natural Resources Conservation Service, 359 p.*

Thompson, S. C., Clague, J. J. & Evans, S. G., 1997: Holocene activity of the Mt. Currie scarp, Coast Mountains, British Columbia, and implications for its origin. *Environ. Eng. Geosci., 3, 329 – 348.*

Tibaldi, A., Rovida, A. & Corazzato, C., 2004: A giant deep-seated slope deformation in the Italian Alps studied by paleoseismological and morphometric techniques. *Geomorphol., 58, 27 – 47.*

Vojtko, R., Marko, F., Preusser, F., Madarás, J. & Kováčová, M., 2011: Late Quaternary fault activity in the Western Carpathians; evidence from the Vikartovce Fault (Slovakia). *Geol. Carpath., 62, 6, 563 – 574.*

Zischinsky, U., 1969: Über sackungen. *Rock Mechanics, 1, 30 – 52.*

APPENDIX 1- Petrographic and diffraction analyses of the fault gouge

Silicate analysis

Analyses results						
		01-004773	01-004774	01-004775	01-004776	01-004777
Component	**Unit**	**PB-1**	**PB-1F**	**PB-2**	**PB-3**	**PB-4**
$Si0_2$	%	60.71	53.38	61.37	61.35	61.06
Al_20_3	%	17.03	18.76	17.16	17.42	17.53
Fe_20_3	%	7.46	9.71	7.19	7.35	7.54
Ca0	%	1.07	1.01	1.09	1.15	1.47
Mg0	%	2.38	2.58	2.41	2.37	2.68
$Ti0_2$	%	0.917	1.073	0.922	0.906	0.912
Mn0	%	0.108	0.170	0.107	0.117	0.146
P_20_5	%	0.15	0.17	0.14	0.14	0.16
Na_20	%	2.87	1.1.98	2.70	2.42	2.77
K_20	%	2.96	2.93	3.17	3.09	3.14
Loss on ignition	%	4.09	8.00	3.52	3.44	2.33
H_20	%	1.27	2.89	1.57	0.99	0.48
Rb	ppm	97	115	106	99	101
Sb	ppm	141	122	136	144	182

X-ray phase analysis

Apparatus: URD-6	Radiation: Cu Kα λ=0,154178 nm	Goniometer shift: 0,1° 2Θ
37 kV / 30 mA	Measuring range: 4 -70° 2 Θ	Frequency of scanning: 1 s

Archive number: **li040/01**	Sample designation: **PB-1**
Positive phases:	
Phases with larger content (dominant): Quartz, Illite, Chlorite, Albite,	Phases with minor content (minor):
Likely phases (or very low phases content): Hematite	
Archive number: **li041/01**	Sample designation: **PB-IF**
Positive phases:	
Phases with larger content (dominant): Quartz, Albite, Illite, Chlorite,	Phases with minor content (minor):
Likely phases (or very low phases content): Hematite	
Archive number: **li042/01**	Sample designation: **PB-2**
Positive phases:	
Phases with larger content (dominant): Quartz, Chlorite, Albite, Illite,	Phases with minor content (minor):
Likely phases (or very low phases content): Hematite	
Archive number: **li043/01**	Sample designation: **PB-3**
Positive phases:	
Phases with larger content (dominant): Quartz, Chlorite, Albite, Illite,	Phases with minor content (minor):
Likely phases (or very low phases content): Hematite	
Archive number: **li044/01**	Sample designation: **PB-4**
Positive phases:	
Phases with larger content (dominant): Quartz, Illite, Albite,	Phases with minor content (minor):
Likely phases (or very low phases content): Hematite	

Postglaciálna deformačná história hlboko založených svahových deformácií na južnom svahu Chabenca, Nízke Tatry, Slovensko

Južný svah Chabenca v Nízkych Tatrách je porušený systémom protiklonných rozsadlín, ktoré predstavujú povrchové prejavy hlboko založenej gravitačnej svahovej deformácie. Predchádzajúce štúdie predpokladali, že hlboko založená deformácia so znakmi tečenia sa pomaly vyvíjala smerom k Lomnistej doline v juhovýchodnom smere (Jahn, 1964; Nemčok, 1972; Mahr a Nemčok, 1977). Svahová deformácia Chabenec je súčasťou dlhšieho pruhu podobných gravitačných porúch vyvinutých medzi Chopkom a Prašivou (vzdialenosť 25 km) v granitoidnom masíve tvoriacom hlavný hrebeň Nízkych Tatier (Nemčok, 1982). Približne 38 % hlavného hrebeňa je tu postihnutých týmto typom svahových deformácií. Ich povrchové prejavy vo forme protiklonných rozsadlín sú dobre viditeľné, keďže väčšina z nich sa nachádza nad pásmom lesa v nadmorskej výške zhruba ≥ 1 400 m. V roku 1997 tu spoločný americko-španielsko-slovenský tím pod vedením prof. Jamesa McCalpina z Univerzity Boulder, Colorado, a Pavla Liščáka z ŠGÚDŠ uskutočnil paleoseizmický výskum, zameraný na zistenie mechanizmu vývoja svahovej deformácie a datovanie udalostí, ktoré viedli k vzniku uvedených rozsadlín. Prieskum v teréne zahŕňal výkopy sondážnych rýh vo vytypovaných rozsadlinách, detailný stratigrafický popis sedimentov zachytených v týchto „sedimentačných pasciach“, odber vzoriek na následné laboratórne petrografické zhodnotenie tektonických ílov, odber vzoriek a datovanie organických sedimentov pomocou metódy ^{14}C. Sondážne ryhy boli široké približne 0,6 m, dlhé 4,5 až 7,3 m a hlboké 2,0 až 2,7 m. Východná stena výkopu v každej sondážnej ryhe bola očistená a pomocou lanka bola vyznačená sieť 10 x 10 cm, ktorá slúžila na zhotovenie grafického záznamu o litologickom zložení a vzorkovaní na milimetrový papier v mierke 1 : 15. Odkryté stratigrafické jednotky boli definované na základe farby, textúry a sedimentárnych štruktúr. Pôdne horizonty na sedimentoch (substráte) boli taktiež identifikované a klasifikované v zmysle terminológie horizontov A/B/C používanej v USA. Petrografickú analýzu zabezpečila RNDr. Eva Žáková z ŠGÚDŠ, rádiokarbónové datovanie sa uskutočnilo v NSF (National Science Foundation), v laboratóriu atómovej hmotnostnej spektrometrie na urýchľovacom hmotnostnom spektrometri (Univerzita Arizona, Tucson, USA).

Protiklonné rozsadliny vo vrchných častiach južného svahu Chabenca (nad pásmom lesa) majú približne paralelný priebeh s vrstevnicami a dosahujú dĺžku 300 – 600 m. Celkovo sme identifikovali 9 rozsadlín od najspodnejšej, označenej 1, až po najvyššiu, označenú 9. Vlastný sondážny prieskum sme uskutočnili v protiklonných rozsadlinách 2, 4, 6 a 7, ktoré mali dĺžku 600 m, 350 m, 300 m a 300 m (v uvedenom poradí). Vertikálny povrchový skok v uvedených dominantných rozsadlinách varíroval v intervale od 1 až do 10 m.

Aplikovali sme paleoseizmickú metódu v štyroch sondážnych ryhách. Uvedenými sondážnymi ryhami realizovanými naprieč tromi protiklonnými trhlinami – rozsadlinami – na južnom hrebeni Chabenca bola odkrytá komplexná strižná zóna v granodiorite ďumbierskeho typu s mylonitmi hrubými 25 – 50 cm so smerom a sklonom 360/55 – 60° (do svahu). Strižné zóny obsahujú viacnásobné zlomové úseky, zóny tektonického ílu a alteračné zóny. Na základe toho je možné predpokladať, že prebiehajúca hlboko založená gravitačná deformácia využíva staré predkvartérne poruchové zóny. Štruktúra a stratigrafia odhalená sondážnymi ryhami sú v súlade s epizodickým sklzom pozdĺž porúch gravitačnej deformácie, spojených s následnou depozíciou a tvorbou pôdy v priľahlých rozsadlinách. Rýchle zmeny v sedimentačnom štýle a prerušenie tvorby pôdy stratigraficky korelujú s epizódami posunov na štruktúrach hlboko založenej gravitačnej deformácie. Napriek zjavnému chronologickému súladu medzi epizodickými pohybmi a tvorbou sedimentov sme sa stretli s ťažkosťami pri rádiokarbónovom datovaní pomocou metódy ^{14}C. Päť z našich 20 vzoriek prinieslo prevrátený vek, a to buď v dôsledku recyklácie starého uhlíka v rozsadlinách, alebo kontaminácie pórovitých starých sedimentov uhlíkom z prekrývajúcich, mladších sedimentov. Nie je vylúčené, že do depresií boli deponované sedimenty z povrchu v obrátenom poradí tak, ako boli erodované (najskôr mladšie a postupne staršie). Sedimenty si takýmto mechanizmom priniesli aj uhlíky a dnes vidíme obrátený vek. Keďže každá rozsadlina obsahovala jednu alebo viac preliačin, ktoré fungovali ako sedimentačné pasce, v spätnom pohľade by bolo vhodné rádiokarbónové datovanie doplniť luminiscenčným datovaním. V čase realizácie uvedených terénnych prác však táto metóda bola ešte len v plienkach a „projekt Chabenec“ s jej aplikáciou nepočítal.

Datovanie metódou ^{14}C vo všetkých štyroch sondážnych ryhách naznačuje, že v neskorom holocéne nastal posun (v období pred 1 410 až 1 860 rokmi). Najdlhší datovaný záznam v jednej sondážnej ryhe (ryha 2) obsahoval štyri odvodené udalosti posunu počas posledných 6 000 rokov, z čoho je zrejmé dlhodobé opakovanie udalosti s periódou v priemere zhruba 1,5 ka. Tieto štyri udalosti vytvorili protiklonnú rozsadlinu s približne 5 m vertikálnym povrchovým posunom. Kvázi synchrónnosť neskorých holocénnych posunov je v kontraste s inými

vo svete známymi lokalitami starých, hlboko založených gravitačných svahových deformácií, kde s narastajúcou nadmorskou výškou sa posuny stávajú mladšími, zrejme v dôsledku relaxácie napätí po ústupe ľadovcov. Takmer synchrónne udalosti posunov vo viacerých nadmorských výškach naznačujú externý spúšťač, či už klimatický, alebo seizmický.

Doručené / Received: 29. 4. 2019
Prijaté na publikovanie / Accepted: 4. 6. 2019